PHYSICAL REVIEW B VOLUME 27, NUMBER 12 15 JUNE 1983

Fully macroscopic description of electrical conduction in metal-insulator-semiconductor structures

M. G. Ancona* and H. F. Tiersten
Department of Mechanical Engineering, Aeronautical Engineering, and Mechanics, Rensselaer Polytechnic Institute, Troy, New York 12181
(Received 15 April 1982)

In an earlier paper [Phys. Rev. B 26, 6104 (1980)], a fully macroscopic description of semiconductors was presented which, in addition to the usual diffusion-drift current equations, includes two new boundary conditions resulting from the requirement that the conservation of linear momentum of the electron and hole fluids be satisfied at semiconductor interfaces. In the present work, this description is applied to situations involving semiconductors which abut insulators, e.g., metal-insulator-semiconductor structures, in which macroscopic currents flow. Consistent boundary conditions for the limiting cases of small signals and low-level injection are derived from the general boundary conditions of the earlier work. To illustrate the use of these conditions, they, together with the familiar small signal and low-level differential equations, are employed in the study of two experiments, namely steady-state photoconductivity and metal-oxide-semiconductor (MOS) admittance. The analysis of the former shows that for dc situations the two semiconduction boundary conditions may be approximated by a single "outer" condition to be applied at the outer edge of the space-charge region. For small signal cases, but *not* for low-level situations, this condition is shown to be well approximated by the often used surface recombination velocity condition (s constant). An expression for the surface recombination velocity in terms of macroscopic surface coefficients is derived, and its predicted variation with bias is in qualitative agreement with known results. For the MOS admittance experiment a similar "outer" condition approach is shown to be inadequate. The purely small signal (linear) treatment given constitutes the field description underlying equivalent circuit representations of the MOS capacitor. Approximate solutions for the admittance are obtained in terms of the macroscopic surface coefficients and are found to be in qualitative agreement with published data.

I. INTRODUCTION

A fully macroscopic description of bounded semiconductors has recently been presented.[1] In that paper the usual diffusion-drift current description of a semiconductor was derived from well-established macroscopic physical principles. Integral forms of the governing equations were exhibited, and a consistent set of boundary conditions was deduced from these forms. Of greatest significance are two new boundary conditions, which arise from the integral forms of the force-balance equations for the electron and hole fluids. These two *semiconduction* boundary conditions relate the jump discontinuities in the chemical potentials across the semiconductor interface to the forces per unit charge density per unit area exerted by the lattice on the charge carriers at the surface. The two conditions were employed in Ref. 1 in the description of the static (or equilibrium) situation in a one-dimensional metal-insulator-semiconductor (MIS) structure. The present paper extends the previous work to discuss the macroscopic description of such structures in situations in which macroscopic currents flow.

The macroscopic description of a semiconductor as obtained in Ref. 1 consists of force (per unit charge) and charge-balance equations for the electron and hole fluids (possibly balance laws for the lattice, which are usually not needed), Gauss's law of electrostatics, the definition of electric potential plus the boundary conditions on the electric potential and the total current, the definition of surface charge, and the new pair of boundary conditions on the electron and hole chemical potentials. With the addition of constitutive relations specifying various material properties, e.g., $\vec{D}=\epsilon\vec{E}$, the system of equations becomes determinate and the field description complete. Included in this specification of material properties are constitutive relations chosen for the surface forces per unit charge density per unit area

that appear in the chemical potential boundary conditions.[2] For the static situation treated in Ref. 1 specific forms were selected containing material coefficients that completely characterize the interface in the absence of dissipation (henceforth termed recoverable coefficients). In the present work, in which carrier fluid velocities are nonzero, additional terms containing material surface coefficients characteristic of dissipative aspects of interfacial response arise in the force expressions. The full set of surface coefficients—recoverable plus dissipative—comprises the complete macroscopic description of the interface. As with other material coefficients, e.g., dielectric constants and mobilities, surface coefficients that, in principle, can be calculated from more fundamental quantum-mechanical models are, in practice, to be measured experimentally. (The familiar reasons for this in the case of bulk coefficients are even more compelling for surface coefficients in view of the microscopic complexity of semiconductor interfaces.) In Ref. 1 the determination from published experimental data of recoverable coefficients for particular semiconductor-insulator interfaces was illustrated. Likewise, an object of this paper is to illustrate the use of experimental data in determining dissipative surface coefficients. When the surface coefficients are known, a detailed and precise understanding of the effects of surfaces on the behavior of device structures may be obtained by solving appropriate boundary-value problems.

In the formulation of time-dependent problems either for measurement or prediction purposes, it is helpful to employ some important limiting forms of the field description that are derived in Sec. II by expanding the dependent field variables about a static biasing state. In this way we obtain the familiar time-dependent "excess-carrier," low-level injection, and small-signal differential equations.[3] In precisely the same manner corresponding versions of the boundary conditions are found. The technique for obtaining these superposed dynamic equations is, of course, standard; however, no such derivations of boundary conditions for either the low-level injection or small-signal situations exist in the literature. This consistent treatment of all equations, enabled by the semiconduction boundary conditions introduced in Ref. 1, constitutes one of the major points of the present work.

In the final two sections we apply the fully macroscopic approach to dynamic situations. In particular, we treat two distinct semiconductor experiments; namely the steady-state photoconductivity experiment in Sec. III and the metal-oxide-semiconductor (MOS) admittance measurement in Sec. IV. The former allows us to examine the behavior of the semiconductor-insulator interface under dc conditions, while the latter provides a vehicle for discussing the interface under small-signal ac conditions. In addition, these examples afford an opportunity for comparing our fully macroscopic formalism with some schemes for the description of interfaces that have been used in the past in place of the missing semiconduction boundary conditions.

In the steady-state photoconductivity experiment photogenerated electrons and holes, which carry zero net current in the direction normal to the large faces of a semiconducting layer, alter the measured transverse conductivity parallel to the large faces of the layer. In the course of analyzing the dc "excess-carrier" problem for carrier flow normal to the large surfaces we show that for low-level and small-signal cases when the Debye length is much less than the layer thickness the *two* semiconduction boundary conditions (containing simple choices for the dissipative terms) are well approximated by a *single* asymptotic "outer" condition[4] to be applied at the outer edges of space-charge regions in the solution of the bulk-carrier-flow problem. Such a condition is useful because the contribution of excess carriers in the narrow space-charge regions to the measured transverse conductivity is negligible. In the small-signal case, this "outer" condition, which is not an actual physical boundary condition, is found to be of the form of the surface-recombination velocity condition introduced by Shockley[5] to incorporate "surface-recombination" effects into the diffusion-drift current description. This reduction constitutes the macroscopic field-theoretic justification for the Shockley condition.[6] Significantly, in the low-level injection case, where the Shockley approach is often applied, the derived asymptotic "outer" condition is no longer of the form of the surface-recombination velocity condition. In other words, the Shockley condition (with s constant) contains a small-signal assumption[7] and when used in a low-level case is inconsistent with the differential equations, i.e., it violates conservation of charge-carrier momentum at the interface. For the small-signal case an expression for the surface-recombination velocity is found in terms of static charge densities and surface and bulk material coefficients. Its variation with bias is shown to be in qualitative agreement with published data.

When the Debye length in the dc experiment is not much smaller than the layer thickness (or in large-signal cases) the solution inside the space-charge region becomes essential, and the asymptotic "outer" condition approach, which in the small-signal case leads to the Shockley condition, is clearly invalid or incomplete. Although the thin-layer steady-state photoconductivity experiment is not of

much interest, the general circumstance of needing to solve problems where detail inside space-charge regions adjacent to semiconductor-insulator interfaces is important arises often. In particular, this situation is found in most transient[8] and ac problems involving interfaces (e.g., the situation treated in Sec. IV) as well as in many dc problems such as in metal-oxide-semiconductor field-effect transistor (MOSFET) modeling. The two interface conditions furnished by the new semiconduction boundary conditions are required for such cases. To be sure, workers interested in device modeling solved these problems in the past by supplying various assumed conditions, e.g., a specification of surface charge plus a Shockley-type condition applied *at* the interface.[9] Conditions like these, which perhaps roughly characterize some important surface effects for modeling purposes, are, like the Shockley condition, simply asserted; various questions as to their *macroscopic* source, meaning, consistency, justification, and limitations remain unanswered. As with the surface-recombination velocity condition, connections to the macroscopic theory (particularly for small-signal dc cases) are again possible. However, since there is no agreement in the literature on what conditions are to be assumed and because of our previous analyses and criticisms of assumed surface-charge conditions in Ref. 1 and the surface-recombination velocity condition in Sec. III of this work, we do not give further discussion of any assumed conditions in Sec. IV. A second approach to problems involving space-charge regions near interfaces has been the development and utilization of equivalent circuit models.[10] These have been employed to provide a more precise description of interface effects, most notably for the understanding of small-signal ac behavior in MOS capacitors. We can now treat such problems within a well-defined macroscopic field-theoretic framework.

In the MOS admittance experiment, pioneered by Nicollian and Goetzberger,[11] a static bias plus a small-amplitude ac signal are applied to the gate electrode of a MOS capacitor. The raw data consist of the current across the structure, i.e., the admittance, as a function of bias and frequency. In the past,[11,12] such data were generally interpreted in terms of various quasimicroscopic entities, such as surface-state densities, capture cross sections, and characteristic areas using the above-mentioned equivalent circuits in conjunction with quasimicroscopic Shockley-Read-Hall—type theory. Since these quantities were obtained from essentially macroscopic measurements, they bear no real quantitative relation to actual microscopic information, e.g., microscopic lattice strain at the surface. In contrast, in the fully macroscopic description the data are used to evaluate various macroscopic material surface coefficients that consistently describe the interface while making no assumptions about its microscopic structure. Furthermore, although we examine only the small-signal case, extensions to degenerate, high-field, and non-small-signal cases may readily be made. Lastly, we should note that since the small-signal description given here is the macroscopic linear field theory underlying existing lumped-parameter representations, it is not surprising that many of the calculated results for the circuit parameters appear familiar.

In the analytical description of the small-signal MOS admittance experiment we find that the dissipative terms introduced in the semiconduction boundary conditions on the basis of dc considerations in Sec. III describe many aspects of the ac situation. As one would expect this is especially true at lower frequencies. At higher frequencies other rather general dissipative terms that vanish in the dc case are required in order to accurately account for an observed dependence of surface response on the time rate of change of electron and hole charge densities just inside the interface. With these added terms quantitative agreement becomes possible.

II. THE MACROSCOPIC EQUATIONS FOR THE SEMICONDUCTOR

The time-dependent differential equations for the semiconductor are given in Sec. III of Ref. 1. For completeness we repeat the pertinent ones in the most convenient forms here:

$$\vec{\nabla}(\varphi+\varphi^e)=\vec{\mathrm{E}}^{\,e}\,, \tag{2.1}$$

$$\vec{\nabla}(\varphi+\varphi^h)=\vec{\mathrm{E}}^{\,h}\,, \tag{2.2}$$

$$\frac{\partial\rho^e}{\partial t}+\vec{\nabla}\cdot\vec{\mathrm{J}}^{\,e}=\gamma^e\,, \tag{2.3}$$

$$\frac{\partial\rho^h}{\partial t}+\vec{\nabla}\cdot\vec{\mathrm{J}}^{\,h}=\gamma^h\,, \tag{2.4}$$

$$\vec{\nabla}\cdot\vec{\mathrm{D}}=\rho\,, \tag{2.5}$$

$$\vec{\mathrm{E}}=-\vec{\nabla}\varphi\,, \tag{2.6}$$

$$\rho=\rho^e+\rho^h+\rho^i\,, \tag{2.7}$$

which correspond to (3.26), (3.27), (3.5), (3.6), (3.13), (3.14), and (3.7), respectively, of Ref. 1. The vectors $\vec{\mathrm{E}}^{\,e}$ and $\vec{\mathrm{E}}^{\,h}$ are the resistive forces per unit charge exerted by the lattice on the electron and hole gases, respectively, in the bulk, and φ^e, φ^h, γ^e, and γ^h are the chemical potentials and charge-source densities for the two charged gases. All other symbols take their familiar meanings. For purposes of this paper we assume no bulk trapping, i.e.,

$$\gamma^e = -\gamma^h \ . \tag{2.8}$$

The system consisting of (2.1)–(2.8) becomes determinate with the addition of constitutive equations for $\vec{E}^e$, $\vec{E}^h$, φ^e, φ^h, $\vec{D}$, and γ^e. In particular, assuming $\vec{E}^e = \vec{v}^e/\mu^e$ and $\vec{E}^h = -\vec{v}^h/\mu^h$, where $\vec{v}^e$ and $\vec{v}^h$ are the macroscopic carrier velocities, and assuming $\varphi^e = \varphi^e(\rho^e)$ and $\varphi^h = \varphi^h(\rho^h)$, we may write (2.1) and (2.2) in the standard forms

$$\vec{J}^e = -\mu^e \rho^e \vec{E} - D^e \vec{\nabla} \rho^e \ , \tag{2.9}$$

$$\vec{J}^h = \mu^h \rho^h \vec{E} - D^h \vec{\nabla} \rho^h \ , \tag{2.10}$$

where

$$D^e = -\mu^e \rho^e \frac{\partial \varphi^e}{\partial \rho^e}, \quad D^h = \mu^h \rho^h \frac{\partial \varphi^h}{\partial \rho^h} \ .$$

The usual choice for $\vec{D}$ is $\vec{D} = \epsilon \vec{E}$, where ϵ is the local dielectric constant, and a common selection for γ^e in n-type material is

$$\gamma^e = \frac{\rho_1^h}{\tau_p} - G \ , \tag{2.11}$$

where G is the charge source density due to illumination and τ_p is the "minority-carrier lifetime."

At all interfaces we have the well-known electrostatic boundary conditions

$$[\varphi] = 0 \ , \tag{2.12}$$

$$\vec{n} \cdot \left[\frac{\partial \vec{D}}{\partial t} + \vec{J} \right] = 0 \ , \tag{2.13}$$

and the definition of surface-charge density

$$\vec{n} \cdot [\vec{D}] = \sigma \ , \tag{2.14}$$

which correspond to Eqs. (3.37), (3.35), and (3.33), respectively, of Ref. 1. As in Ref. 1 we have introduced the conventional notation $[C]$ to denote $C^+ - C^-$ with $\vec{n}$ denoting the unit normal directed from the $-$ to $+$ side of the surface of discontinuity.

The semiconduction boundary conditions are[13]

$$[\varphi^e] = f^e(\rho^e, \vec{v}^e, \vec{E}) \ , \tag{2.15}$$

$$[\varphi^h] = f^h(\rho^h, \vec{v}^h, \vec{E}) \ , \tag{2.16}$$

which correspond to Eqs. (3.40) and (3.42), respectively, of Ref. 1. We recall that f^e and f^h are the forces per unit charge density per unit area exerted by the lattice on the carriers at the surface. We also recall that φ^e and φ^h are the chemical potentials for the electron and hole gases, respectively. As constitutive choices for φ^e and φ^h we take the Maxwell gas forms[14]

$$\varphi^e(\rho^e) = -\frac{kT}{q} \ln \left[\frac{\rho^e}{-qN_c} \right] , \tag{2.17}$$

$$\varphi^h(\rho^h) = \frac{kT}{q} \ln \left[\frac{\rho^h}{qN_v} \right] . \tag{2.18}$$

On the basis of forms found useful in the static case treated in Ref. 1 and on evidence discussed in Secs. III and IV of this paper, for Si-SiO_2 interfaces we select the surface-force constitutive equations to be of the form

$$\begin{aligned} f^e = {} & A_0^R + A_1^R \vec{n} \cdot \vec{E}_{\rm ins} + A_2^R \vec{n} \cdot \vec{E}_{\rm sem} \\ & + A_3^R \ln(\rho^e/\rho_b^e) + A_4^R [\ln(\rho^e/\rho_b^e)]^2 + \cdots \\ & + \int_{-\infty}^{t} E(t-s) \frac{\partial \rho^e(s)}{\partial s} ds + \vec{A}^D \cdot \vec{v}^e + \cdots \ , \end{aligned} \tag{2.19}$$

$$\begin{aligned} f^h = {} & D_0^R + D_1^R \vec{n} \cdot \vec{E}_{\rm ins} + D_2^R \vec{n} \cdot \vec{E}_{\rm sem} \\ & - D_3^R \ln(\rho^h/\rho_b^h) + D_4^R [\ln(\rho^h/\rho_b^h)]^2 + \cdots \\ & + \int_{-\infty}^{t} H(t-s) \frac{\partial \rho^h(s)}{\partial s} ds + \vec{D}^D \cdot \vec{v}^h + \cdots \ , \end{aligned} \tag{2.20}$$

where ρ_b^e and ρ_b^h are the electron and hole charge densities at the position where $\varphi = \varphi_{\rm ref} = 0$. Equations (2.19) and (2.20) define the recoverable (A_i^R and D_i^R, $i \geq 0$) and dissipative [$\vec{A}^D$, $\vec{D}^D$, $E(t)$, and $H(t)$] material surface coefficients that together completely characterize the semiconductor interface.[15] In the static case, i.e., when no currents flow, the dissipative terms vanish [we assume $E(t)$ and $H(t) \to 0$ as $t \to \pm\infty$] whereupon the boundary conditions (2.15) and (2.16) with (2.19) and (2.20) reduce to the single condition found in Ref. 1. In making this reduction, relations between the A_i^R and D_i^R coefficients arise. For convenience we have slightly altered the recoverable forms used in Ref. 1 by including auxiliary coefficients A_0^R and D_0^R in (2.19) and (2.20) that as pointed out in Ref. 1, are unnecessary for the description of semiconductor interfaces.[16] If we select

$$A_0^R = \varphi_b^h - \varphi_{\rm ins}^h, \quad D_0^R = \varphi_b^e - \varphi_{\rm ins}^e \ , \tag{2.21}$$

where $\varphi_{\rm ins}^e$ and $\varphi_{\rm ins}^h$ and φ_b^e and φ_b^h are the constant values of the chemical potentials for electrons and holes in the insulator and in the bulk of the semiconductor, respectively, then, as in Ref. 1, we can show that

$$A_i^R = D_i^R, \quad i \geq 1 \ . \tag{2.22}$$

We defer discussion of the reasons for writing the

dissipative terms in (2.19) and (2.20) in the forms shown until Secs. III and IV.

Equations (2.3)–(2.20) with (2.21) and (2.22) constitute the full macroscopic description of a semiconductor subject to the assumptions mentioned in Ref. 1. We are interested in the application of these to two special cases, namely, (i) the small-signal situation and (ii) the low-level injection case for a static biasing state only. The dynamic equations required in both special cases are obtained by expanding all field variables about the static biasing state; thus

$$\varphi=\varphi_0+\varphi_1,\ \rho^e=\rho_0^e+\rho_1^e,\ \rho^h=\rho_0^h+\rho_1^h,$$
$$\varphi^e=\varphi_0^e+\varphi_1^e,\ \varphi^h=\varphi_0^h+\varphi_1^h, \tag{2.23}$$

where the variables with the subscript 0 are the static biasing values and those with the subscript 1 are the dynamic variables. For the small-signal case all static variables in (2.23) are assumed to be much larger than their associated dynamic variables. The low-level injection case makes the same assumption on all variables except for the minority-carrier charge density. It is noted that since the carrier velocities vanish in the static biasing state, the velocities and currents carry only the subscript 1, which we omit. We note that for some applications not considered here it is useful to expand about a steady biasing state, in which case currents and velocities with 0 subscripts would arise; although the resulting dynamic equations would retain the same form, the dynamic boundary conditions would change somewhat.

Employing (2.23) with no assumption on the magnitudes of the dynamic variables along with the usual constitutive relations $\vec{D}=\epsilon_{\rm sem}\vec{E}$ (semiconductor) and $\vec{D}=\epsilon_{\rm ins}\vec{E}$ (insulator) in (2.3)–(2.11) and utilizing the fact that the static form of these equations is satisifed in the usual way, we arrive at the familiar "excess-carrier" equations shown here for n-type material in the form

$$\vec{J}^{\,e}=-\mu^e\rho_1^e\vec{E}_0-\mu^e(\rho_0^e+\rho_1^e)\vec{E}_1-D^e\vec{\nabla}\rho_1^e\ , \tag{2.24}$$

$$\vec{J}^{\,h}=\mu^h\rho_1^h\vec{E}_0+\mu^h(\rho_0^h+\rho_1^h)\vec{E}_1-D^h\vec{\nabla}\rho_1^h\ , \tag{2.25}$$

$$\frac{\partial\rho_1^e}{\partial t}+\vec{\nabla}\cdot\vec{J}^{\,e}=\frac{\rho_1^h}{\tau_p}-G\ , \tag{2.26}$$

$$\frac{\partial\rho_1^h}{\partial t}+\vec{\nabla}\cdot\vec{J}^{\,h}=-\frac{\rho_1^h}{\tau_p}+G\ , \tag{2.27}$$

$$\nabla^2\varphi_1=-\frac{1}{\epsilon_{\rm sem}}(\rho_1^e+\rho_1^h)\ , \tag{2.28}$$

while in the insulator, we have

$$\nabla^2\varphi_1=0\ . \tag{2.29}$$

In precisely the same manner, i.e., by inserting (2.23) into (2.15) and (2.16) and employing the static forms of (2.15) and (2.16), which are satisfied, we find the excess-carrier forms of the new semiconduction boundary conditions,

$$[\varphi_1^e]=f_1^e\ , \tag{2.30}$$

$$[\varphi_1^h]=f_1^h\ , \tag{2.31}$$

where we have written f^e and f^h as static and time-dependent excess-carrier parts, i.e., $f^e\equiv f_0^e+f_1^e$ and $f^h\equiv f_0^h+f_1^h$. For Si-SiO_2 interfaces, from (2.19) and (2.20) with (2.22), we find that f_0^e and f_0^h are given by

$$f_0^e-A_0^R=f_0^h-D_0^R=A_1^R\vec{n}\cdot\vec{E}_0\,|_{\rm ins}+A_2^R\vec{n}\cdot\vec{E}_0\,|_{\rm sem}+A_3^R\bar{\varphi}_0+A_4^R\bar{\varphi}_0^2+\cdots\ , \tag{2.32}$$

where the static relations

$$\varphi_0=(D^e/\mu^e)\ln(\rho_0^e/\rho_b^e)=-(D^h/\mu^h)\ln(\rho_0^h/\rho_b^h)$$

and the definition

$$\bar{\varphi}_0\equiv\mu^e\varphi_0/D^e=\mu^h\varphi_0/D^h$$

have been used. Since (2.32) holds for the static solution, then from (2.19) and (2.20) with (2.22), we obtain

$$f_1^e=A_1^R\vec{n}\cdot\vec{E}_1\,|_{\rm ins}+A_2^R\vec{n}\cdot\vec{E}_1\,|_{\rm sem}+\tilde{A}^S\left[\ln\left[1+\frac{\rho_1^e}{\rho_0^e}\right]\right]+A_4^R\left[\ln\left[1+\frac{\rho_1^e}{\rho_0^e}\right]\right]^2+\cdots$$
$$+\int_{-\infty}^{t}E(t-s)\frac{\partial\rho_1^e(s)}{\partial s}ds-\frac{\vec{n}\cdot\vec{J}^{\,e}}{\nu^e(\rho_0^e+\rho_1^e)}+\cdots\ , \tag{2.33}$$

$$f_1^h=A_1^R\vec{n}\cdot\vec{E}_1\,|_{\rm ins}+A_2^R\vec{n}\cdot\vec{E}_1\,|_{\rm sem}-\tilde{A}^S\left[\ln\left[1+\frac{\rho_1^h}{\rho_0^h}\right]\right]+A_4^R\left[\ln\left[1+\frac{\rho_1^h}{\rho_0^h}\right]\right]^2+\cdots$$
$$+\int_{-\infty}^{t}H(t-s)\frac{\partial\rho_1^h(s)}{\partial s}ds+\frac{\vec{n}\cdot\vec{J}^{\,h}}{\nu^h(\rho_0^h+\rho_1^h)}+\cdots\ , \tag{2.34}$$

as the constitutive relations for the excess-carrier portions of the surface forces, where

$$\tilde{A}^S = A_3 + 2A_4\bar{\varphi}_0 + \cdots .$$

In reaching (2.33) and (2.34), we have assumed

$$\vec{A}^D = -\vec{n}/\nu^e, \quad \vec{D}^D = \vec{n}/\nu^h , \tag{2.35}$$

since we expect the normal forces f_1^e and f_1^h to be linked most closely with the normal components of $\vec{J}^e$ and $\vec{J}^h$. The quantities ν^e and ν^h may be called the scalar surface "receptivity" coefficients for the electron and hole gases, respectively. Lastly, expanding (2.12)—(2.14) according to (2.23) and utilizing the fact that the static portions of the equations are satisfied, we obtain

$$[\varphi_1] = 0 , \tag{2.36}$$

$$\vec{n}\cdot\left[\frac{\partial\vec{D}_1}{\partial t} + \vec{J}\right] = 0 , \tag{2.37}$$

$$\vec{n}\cdot[\vec{D}_1] = \sigma_1 , \tag{2.38}$$

where σ_1 is the excess-carrier surface charge density. Equations (2.24)—(2.31) and (2.33)—(2.38) are the excess-carrier equations for the semiconductor subject to various restrictions mentioned above.

As noted earlier, the small-field description is found by expanding (2.24)—(2.38) under the assumptions that $y_0 \gg y_1$, where y is any of ρ^e, ρ^h, or φ, and that the velocities (or currents) are small, thus retaining only lowest-order terms. The familiar small-signal differential equations merely drop the terms $\mu^e\rho_1^e\vec{E}_1$ and $\mu^h\rho_1^h\vec{E}_1$ from (2.24) and (2.25), while all boundary conditions remain the same except the semiconduction conditions (2.30) and (2.31) with (2.33) and (2.34), respectively. For the semiconduction boundary conditions we expand (2.30) with (2.17) and (2.33), and (2.31) with (2.18) and (2.34) (assuming φ_{ox}^e and φ_{ox}^h to be constants) while retaining only linear terms to obtain the small-signal, semiconduction boundary conditions

$$0 = A_1^R\vec{n}\cdot\vec{E}_1\,|_{ins} + A_2^R\vec{n}\cdot\vec{E}_1\,|_{sem} + \frac{\rho_1^e}{\rho_0^e}A^s + \int_{-\infty}^{t} E(t-s)\frac{\partial\rho_1^e(s)}{\partial s}ds - \frac{\vec{n}\cdot\vec{J}^e}{\nu^e\rho_0^e} , \tag{2.39}$$

$$0 = A_1^R\vec{n}\cdot\vec{E}_1\,|_{ins} + A_2^R\vec{n}\cdot\vec{E}_1\,|_{sem} - \frac{\rho_1^h}{\rho_0^h}A^s + \int_{-\infty}^{t} H(t-s)\frac{\partial\rho_1^h(s)}{\partial s}ds + \frac{\vec{n}\cdot\vec{J}^h}{\nu^h\rho_0^h} , \tag{2.40}$$

where

$$A^s \equiv \tilde{A}^s - kT/q .$$

The important low-level injection equations can be found in a similar manner except that the dynamic minority-carrier density is not assumed to be small in making the expansions. Since we wish to consider inversion layers the consequences of the assumption on the minority-carrier density may vary over the region of interest. For this reason, we do not present those equations, noting only that for an accumulation-depletion situation in n-type material, the appropriate boundary conditions are (2.39) and (2.31) with (2.34).

It should again be emphasized that because two boundary conditions were missing from the conventional diffusion-drift current description of semiconductors, the consistent treatment of the *entire* description in deducing the forms for the special cases discussed above was heretofore impossible, and while the differential equations found are well known, the derived boundary conditions for the special cases considered are new. In addition, we note that just as the bulk recoverable coefficients D^e/μ^e and D^h/μ^h contribute strongly to the dynamic characteristics in any of the above cases through their appearance in (2.24) and (2.25), so also do the recoverable coefficients A_i^R in (2.33) and (2.34). Moreover, the solution to the static problem, that is, $\rho_0^e(x)$, $\rho_0^h(x)$, and $E_0(x)$, have significant influence on the dynamic characteristics both through the differential equations (2.24) and (2.25) *and* through the boundary conditions (2.30) with (2.33) and (2.31) with (2.34). Of course, material coefficients solely characteristic of the dissipative behavior, i.e., μ^e, μ^h, ν^e, ν^h, $E(t)$, and $H(t)$, also have a crucial influence on the dynamic characteristics.

We close this section by noting that the semiconduction boundary conditions for both static and dynamic situations may be rephrased in a somewhat more convenient form. As discussed in Ref. 1 the static boundary condition found by inserting (2.21), (2.22), and (2.32) into the static forms of either (2.15) or (2.16) may be rewritten by employing the static version of (2.14) and the linear constitutive relation for $\vec{D}$, multiplying through by ϵ_{ins}/A_1^R, and rearranging terms to find the condition

$$\vec{n}\cdot[\vec{D}_0] = \sigma_0 = B_0 + B_1\left.\frac{d\varphi_0}{dx}\right|_{sem} + B_2\varphi_0 + B_3\varphi_0^2 + \cdots , \tag{2.41}$$

where

$$B_0=-\frac{\epsilon_{\rm ins}}{A_1^R}(\varphi_b^h-\varphi_{\rm ins}^h+\varphi_b^e-\varphi_{\rm ins}^e)\ ,$$

$$B_1=-\left[\epsilon_{\rm sem}+\epsilon_{\rm ins}\frac{A_2^R}{A_1^R}\right]\ ,$$

$$B_2=-\frac{\epsilon_{\rm ins}}{A_1^R}\left[\frac{\mu^e}{D^e}A_3^R-1\right]\ ,$$

$$B_i=-\frac{\epsilon_{\rm ins}A_{i+1}^R}{A_1^R}\left[\frac{\mu^e}{D^e}\right]^{i-1}\ ,\quad i\geq 3\ .$$

Now if in addition we define

$$\beta^e=A_1^R\nu^e/\epsilon_{\rm ins},\quad \beta^h=A_1^R\nu^h/\epsilon_{\rm ins}\ ,$$

$$e(t)=-\mu^e\epsilon_{\rm ins}E(\epsilon)/A_1^RD^e\ ,$$

$$h(t)=-\mu^e\epsilon_{\rm ins}H(t)/A_1^RD^e\ ,$$

then the excess-carrier conditions (2.30) with (2.33) and (2.31) with (2.34) may be recast completely in terms of these auxiliary coefficients with no explicit dependence on $\Delta\equiv\varphi_b^h-\varphi_{\rm ins}^h+\varphi_b^s-\varphi_{\rm ins}^e$. The ability to make this transformation is significant because it is the auxiliary parameters that are actually determined from experimental measurement, and therefore the entire description, whether written in terms of the A_i^R, ν^e, ν^h, $E(t)$, and $H(t)$ coefficients or with the B_i parameters, is independent of Δ, a quantity which is not accurately known. It should be emphasized, however, that it is the A_i^R, ν^e, ν^h, $E(t)$, and $H(t)$ coefficients and not the derived coefficients that are material parameters characteristic of a particular interface since the latter depend on bulk as well as surface parameters. In order to find the fundamental A_i coefficients we have assumed $\Delta\approx 8.5$ V (Ref. 17) in this paper.

III. APPLICATION TO SEMICONDUCTOR-INSULATOR INTERFACES UNDER STEADY dc CONDITIONS

As mentioned in the Introduction the steady-state photoconductivity experiment provides a situation requiring an analytical treatment of semiconductor-insulator interfaces using the fully macroscopic description under dc conditions. In addition, it furnishes a circumstance in which the two semiconduction boundary conditions presented in Ref. 1 and given in (2.15) and (2.16) with (2.19) and (2.20) of this work can be compared with and related to the conventional treatment involving the surface-recombination velocity condition. Furthermore, the steady-state photoconductivity experiment provides a specific illustration of how experiments may be used to determine dissipative surface coefficients. We begin with a brief discussion of the experiment.[18]

The experimental apparatus commonly used (in the past) in surface-recombination experiments consists of a planar insulator-semiconductor-insulator sandwich to which contact electrodes are attached at opposite ends of the semiconductor layer (filament) and transverse electrodes are fixed on the broad insulator faces, as shown in Fig. 1. In the steady-state photoconductivity experiment, constant and spatially uniform illumination of the semiconductor generates electron-hole pairs that travel (chiefly) to the broad insulated surfaces where they are absorbed at a rate equal to the generation rate. The increase in carrier density over the dark condition is thus a measure of the dc characteristics of the interface and may be monitored by measuring the transverse dc conductivity for current flow between the end-contact electrodes. Application of a static voltage to the transverse electrodes allows the static (dark) state to be varied. Since the experimental conditions are chosen so as to minimize end effects, e.g., sweep out, we may, as is normally done,[19] regard this two-dimensional (at least) problem as being two one-dimensional problems: (i) the calculation of the added-carrier density and (ii) the calculation of the dc transverse conductivity given the solution to (i). In this paper we treat only the former problem and use existing results for the latter.[20]

The added-carrier problem (i) is modeled as shown in Fig. 2. We take the solution to the static one-dimensional problem with potential φ_A applied at the transverse electrodes, i.e., $\rho_0^e(x)$, $\rho_0^h(x)$, and $\varphi_0(x)$, which is found using the static boundary condition (2.15) with (2.32) as in Ref. 1, to be known. We note that this static solution has a boundary-layer character with φ_0 and the total charge density ρ_0 being zero everywhere outside of narrow space-charge or Debye regions, which exist adjacent to the semiconductor surfaces. The equa-

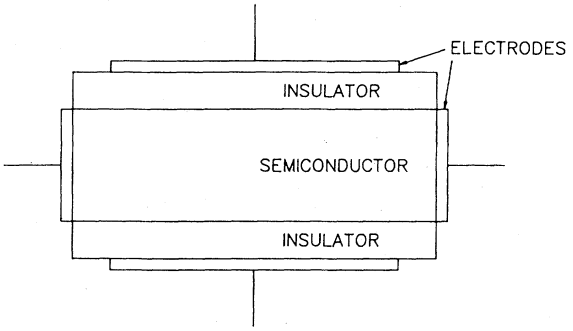

FIG. 1. Schematic diagram of the structure used in the steady-state photoconductivity experiment.

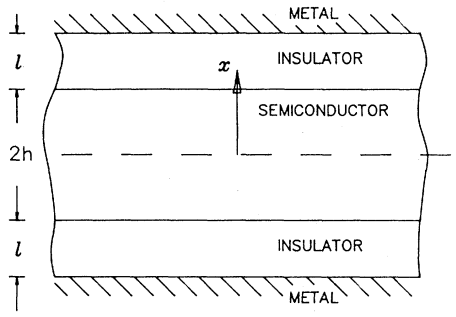

FIG. 2. Schematic diagram of the one-dimensional added-carrier problem.

tions descriptive of the flow of the photogenerated carriers normal to the insulated faces are then the excess-carrier differential equations (2.24)–(2.29) written for a one-dimensional steady-state situation with constant illumination. For n-type material these are

$$J^e=\mu^e\rho_1^e\frac{d\varphi_0}{dx}+\mu^e(\rho_0^e+\rho_1^e)\frac{d\varphi_1}{dx}-D^e\frac{d\rho_1^e}{dx},\quad |x|\le h \tag{3.1}$$

$$J^h=-\mu^h\rho_1^h\frac{d\varphi_0}{dx}-\mu^h(\rho_0^h+\rho_1^h)\frac{d\varphi_1}{dx}-D^h\frac{d\rho_1^h}{dx},\quad |x|\le h \tag{3.2}$$

$$\frac{dJ^e}{dx}=\frac{\rho_1^h}{\tau_p}-G,\quad |x|\le h \tag{3.3}$$

$$\frac{dJ^h}{dx}=-\frac{\rho_1^h}{\tau_p}+G,\quad |x|\le h \tag{3.4}$$

$$\frac{d^2\varphi_1}{dx^2}=-\frac{1}{\epsilon_{\text{sem}}}(\rho_1^e+\rho_1^h),\quad |x|\le h \tag{3.5}$$

$$\frac{d^2\varphi_1}{dx^2}=0,\quad h<|x|<h+l \tag{3.6}$$

where we recall that G is the charge-source density due to the illumination. For the one-dimensional steady-state case the excess-carrier boundary conditions (2.30)–(2.37) linearized in the velocities[21] take the forms

$$\mp A_1\frac{d\varphi_1}{dx}\bigg|_{\text{ins}}\mp A_2\frac{d\varphi_1}{dx}\bigg|_{\text{sem}}+A^S\ln\left[1+\frac{\rho_1^e}{\rho_0^e}\right]+A_4\ln^2\left[1+\frac{\rho_1^e}{\rho_0^e}\right]+\cdots\pm\frac{J^e}{\nu^e\rho^e}=0\ \text{ at }\ |x|=h \tag{3.7}$$

$$\mp A_1\frac{d\varphi_1}{dx}\bigg|_{\text{ins}}\mp A_2\frac{d\varphi_1}{dx}\bigg|_{\text{sem}}-A^S\ln\left[1+\frac{\rho_1^h}{\rho_0^h}\right]+A_4\ln^2\left[1+\frac{\rho_1^h}{\rho_0^h}\right]+\cdots\mp\frac{J^h}{\nu^h\rho^h}=0\ \text{ at }\ |x|=h \tag{3.8}$$

$$J^e+J^h=0\ \text{ at }\ |x|=h\ , \tag{3.9}$$

$$[\varphi_1]=0\ \text{ at }\ |x|=h\ , \tag{3.10}$$

$$\varphi_1=0\ \text{ at }\ |x|=h+l\ , \tag{3.11}$$

where, for convenience, we have omitted the R superscripts in (3.7) and (3.8). By subtracting (3.7) from (3.8) we may derive a useful alternate semiconduction boundary condition that is explicitly independent of the electric fields on either side of the interface. Thus

$$A^S\left[\ln\left[1+\frac{\rho_1^e}{\rho_0^e}\right]+\ln\left[1+\frac{\rho_1^h}{\rho_0^h}\right]\right]+A_4\left[\ln^2\left[1+\frac{\rho_1^e}{\rho_0^e}\right]-\ln^2\left[1+\frac{\rho_1^h}{\rho_0^h}\right]\right]+\cdots\pm\frac{J^e}{\nu^e\rho^e}\pm\frac{J^h}{\nu^h\rho^h}=0\ \text{ at }\ |x|=h \tag{3.12}$$

which, of course, may be substituted for either (3.7) or (3.8). Equations (3.1)–(3.6), (3.9)–(3.11), and any two of (3.7), (3.8), and (3.12) constitute a well-posed boundary-value problem in the macroscopic theory of semiconductors that may be solved for φ_1 at all $|x|\le h+l$ and ρ_1^e, ρ_1^h, J^e, and J^h for $|x|\le h$. From the calculated added-carrier densities $\rho_1^e(x)$ and $\rho_1^h(x)$, one could then set up the transverse conductivity problem (ii), the solution of which in conjunction with experiment would enable the determination of the unknown dissipative surface coefficient ν^e and/or ν^h.

As indicated in the Introduction, in discussing the problem (3.1)–(3.12), it is helpful to distinguish two

cases, viz., $L \ll h$ (where L is the thickness of the Debye region) and $L \not\ll h$. In the former case, several standard approximations may be applied that considerably simplify the analysis; in the latter these approximations are not valid, and it is necessary to consider the full problem, which is, of course, applicable regardless of the relative sizes of L and h. Because the case for which $L \not\ll h$ is of far less experimental interest, it will not be explored in this paper.

Before presenting the approximate analysis of (3.1)–(3.12) in the case $L \ll h$ we briefly describe the conventional continuum approach for the case $L \ll h$ as applied to the steady-state photoconductivity experiment. To begin we note that if $L \ll h$, then, following standard procedures, the second derivative of φ_1 in (3.5) is negligible outside the space-charge region, and we have the familiar "charge-neutrality" approximation[22]

$$\rho_1^e = -\rho_1^h, \quad |x| < h - L \ . \tag{3.13}$$

Now, since $d\varphi_0/dx$, ρ_0^e, and ρ_0^h are constants, the elimination of ρ_1^e, $d\varphi_1/dx$, J^e, and J^h from (3.1)–(3.4) and (3.13) yields a single second-order equation for ρ_1^h in the region $|x| < h - L$, which takes the form

$$\frac{d^2\rho_1^h}{dx^2}\left[\frac{1}{\rho_b^e}-\frac{1}{\rho_b^h}\right]=\left[\frac{\rho_1^h}{\tau_p}-G\right]\left[\frac{1}{D^e\rho_b^e}-\frac{1}{D^h\rho_b^h}\right], \quad |x| < h - L \ . \tag{3.14}$$

Clearly, a single pair of conditions (which do not contain φ_1) supplied at $|x| = h - L$ would be sufficient to solve for ρ_1^h $(= -\rho_1^e)$ in the charge-neutral region. The surface-recombination velocity condition introduced by Shockley[5] provides just such a pair of conditions. These are

$$J^h = \pm s\rho_1^h \text{ at } |x| = h - L \ , \tag{3.15}$$

where s is the surface-recombination velocity, a parameter presumed to characterize the semiconductor interface. One additional simplification used for extrinsic material is that since $-\rho_0^e \gg \rho_0^h$ (for n type), (3.14) may be approximated as

$$D^h\frac{d^2\rho_1^h}{dx^2}=\frac{\rho_1^h}{\tau_p}-G, \quad |x| < h - L \tag{3.16}$$

which with (3.15) is easily solved for ρ_1^h. Thus the added-carrier problem in the charge-neutral region (but *not* in the space-charge regions) can be solved[23]; if we ignore (or assume values for) the added-carrier densities in the space-charge regions, then we possess the required information for the transverse conductivity calculation from which s can be measured.

The surface-recombination velocity condition (3.15) has proven to be quite useful for interpreting the results of many experiments investigating semiconductor surfaces,[24] and it has provided considerable understanding of the influence of surfaces on the behavior of devices.[25] Nonetheless, the Shockley condition (3.15), unlike the semiconduction boundary conditions (3.7) and (3.8), is merely a condition supplied to enable one to solve the charge-neutral form of the excess-carrier equations. As noted in the Introduction it is not deduced as the excess-carrier version of some physically defined boundary conditions, and no clear macroscopic statement of its source, meaning (e.g., relation of s to actual macroscopic surface properties[26]), justification,[7] and limitations[27] is given. Among the consequences of these points is that we have no rational way of extending the Shockley technique to solve problems in space-charge regions. As previously mentioned, the boundary-value problem (3.1)–(3.12) circumvents these difficulties.

We now return to the approximate treatment of the problem specified in (3.1)–(3.12) in the case when $L \ll h$. In view of the foregoing we observe that since the contribution of the added carriers in the space-charge regions to the transverse conductivity is negligible, one would like to deduce from (3.7), (3.8), and (3.12) conditions—perhaps the Shockley conditions (3.15)—to be imposed at $|x| = h - L$ for solutions of the charge-neutral problem, thereby avoiding the (difficult) space-charge region portion of the problem embodied in (3.1)–(3.12). To this end, it is first necessary to recognize that in making the charge-neutrality approximation, a second derivative of φ_1 [in (3.5)] was dropped, which lowered the order of the differential system by two.[28] As a result, the charge-neutral form of the equations, i.e., (3.1)–(3.4) and (3.13), cannot, in general, satisfy two of the boundary conditions. In particular, because it is a second derivative of φ_1 that is dropped, the conditions containing the normal derivative of φ_1 must go unsatisifed, i.e., (3.7) or (3.8) but not (3.12). And, consequently, we seek to obtain from (3.12) a pair of "outer" conditions to be applied to the charge-neutral problem.[29]

The connection between (3.12) and conditions at $|x| = h - L$ is reached essentially by arguing that as far as the excess-carrier equations are concerned, the space-charge region may be regarded as being of zero thickness. From (3.1) and (3.2) with the aid of the static solution relating the variables ρ_0^e, ρ_0^h, and φ_0, we obtain

$$\frac{d}{dx}\left[\varphi_1-\frac{D^e}{\mu^e}\ln\left[1+\frac{\rho_1^e}{\rho_0^e}\right]\right]=\frac{v^e}{\mu^e} \ , \tag{3.17}$$

$$\frac{d}{dx}\left[\varphi_1-\frac{D^h}{\mu^h}\ln\left[1+\frac{\rho_1^h}{\rho_0^h}\right]\right]=-\frac{v^h}{\mu^h} \ . \tag{3.18}$$

Then integrating (3.17), (3.18), (3.3), and (3.4) across the boundary layer (here the Debye region near $x=h$), we find

$$\left[\varphi_1-\frac{D^e}{\mu^e}\ln\left[1+\frac{\rho_1^e}{\rho_0^e}\right]\right]_{h-L}^{h^-}=\int_{h-L}^{h^-}\frac{v^e}{\mu^e}dx\ , \tag{3.19}$$

$$\left[\varphi_1+\frac{D^h}{\mu^h}\ln\left[1+\frac{\rho_1^h}{\rho_0^h}\right]\right]_{h-L}^{h^-}=-\int_{h-L}^{h^-}\frac{v^h}{\mu^h}dx\ , \tag{3.20}$$

$$[J^e]_{h-L}^{h^-}=-[J^h]_{h-L}^{h^-}=\int_{h-L}^{h^-}\left[\frac{\rho_1^h}{\tau_p}-G\right]dx\ . \tag{3.21}$$

When L is small the right-hand sides of these equations are negligible,[30] and the resulting relations express the familiar assumptions of constant electrochemical potentials and current densities across the space-charge layer as seen, for example, in the classic treatment of the p-n junction.[5] Now, by combining (3.19) and (3.20) (with right-hand sides neglected) we find

$$\left[\ln\left[1+\frac{\rho_1^e}{\rho_0^e}\right]+\ln\left[1+\frac{\rho_1^h}{\rho_0^h}\right]\right]_{h^-}\cong\left[\ln\left[1+\frac{\rho_1^e}{\rho_0^e}\right]+\ln\left[1+\frac{\rho_1^h}{\rho_0^h}\right]\right]_{h-L}\ . \tag{3.22}$$

To proceed further we next restrict our attention to the low-level injection and small-signal cases. For n-type material the low-level assumptions at $x=h-L$ are $-\rho_0^e\gg-\rho_1^e,\rho_0^h,\rho_1^h$, under which the right-hand side of (3.22) is approximated by $\ln(1+\rho_1^h/\rho_0^h)$. For the left-hand side of (3.22) we consider three cases that encompass all possible nondegenerate surface conditions: accumulation-depletion, $-\rho_0^e\gg-\rho_1^e,\rho_0^h,\rho_1^h$, near intrinsic, $-\rho_0^e,\rho_0^h\gg-\rho_1^e,\rho_1^h$, and inversion, $\rho_0^h\gg\rho_1^h,-\rho_0^e,-\rho_1^e$. The low-level forms for (3.22) are then

$$\ln\left[1+\frac{\rho_1^h}{\rho_0^h}\right]\Bigg|_{h^-}\cong\ln\left[1+\frac{\rho_1^h}{\rho_0^h}\right]\Bigg|_{h-L} \tag{3.23a}$$

for the accumulation-depletion case,

$$\left[\frac{\rho_1^e}{\rho_0^e}+\frac{\rho_1^h}{\rho_0^h}\right]_{h^-}\cong\ln\left[1+\frac{\rho_1^h}{\rho_0^h}\right]\Bigg|_{h-L} \tag{3.23b}$$

for the near-intrinsic case, and

$$\ln\left[1+\frac{\rho_1^e}{\rho_0^e}\right]\Bigg|_{h^-}\cong\ln\left[1+\frac{\rho_1^h}{\rho_0^h}\right]\Bigg|_{h-L} \tag{3.23c}$$

for the inversion case. For small-signal cases certain obvious further reductions can be made.

Employing (3.23) (plus an identical set at $x=L-h$) and the fact that for the steady state $J^e(x)=-J^h(x)$, $|x|\le h$ [as may be deduced from (3.3), (3.4), and (3.9)] in the semiconduction boundary condition (3.12), we arrive at

$$J^h\cong\pm\frac{A_s^s\ln(1+\rho_1^h/\rho_0^h)-A_4\ln^2(1+\rho_1^h/\rho_0^h)+\cdots}{(1/\nu^e\rho_s^e)-1/\nu^h\rho_s^h(1+\rho_1^h/\rho_0^h)}\quad\text{at } |x|=h-L \tag{3.24a}$$

$$J^h\cong\pm\frac{A_s^s\rho_1^h/\rho_0^h}{(1/\nu^e\rho_s^e)-1/\nu^h\rho_s^h}\quad\text{at } |x|=h-L \tag{3.24b}$$

$$J^h\cong\pm\frac{A_s^s\ln(1+\rho_1^h/\rho_0^h)+A_4\ln^2(1+\rho_1^h/\rho_0^h)+\cdots}{1/\nu^e\rho_s^e(1+\rho_1^h/\rho_0^h)-1/\nu^h\rho_s^h}\quad\text{at } |x|=h-L \tag{3.24c}$$

which are valid for the accumulation-depletion, near-intrinsic, and inversion regimes, respectively. The s subscripts indicate quantities evaluated at $|x|=h^-$, e.g., $\rho_s^e\equiv\rho_0^e(|x|=h^-)$. Equations (3.24) are the asymptotic "outer" conditions we have been looking for, which are written here for the low-level injection case. We note that they are not of the simple form of the surface-recombination velocity conditions (3.15), which are often used in the low-level injection case. The above anlaysis indicates that this use is unjustified. Implications of this point will be explored later, but first we further simplify the equations in (3.24).

Since in the accumulation-depletion regime $-\rho_s^e\gg\rho_s^h$, $|\nu^e\rho_s^e|$ is often much greater than $|\nu^h\rho_s^h(1+\rho_1^h/\rho_0^h)|$, and hence (3.24a) may be approximated by

$$J^h \cong \mp \nu^h \rho_s^h \left[1+\frac{\rho_1^h}{\rho_0^h}\right]\left[A_s^s \ln\left[1+\frac{\rho_1^h}{\rho_0^h}\right]-A_4 \ln^2\left[1+\frac{\rho_1^h}{\rho_0^h}\right]+\cdots\right] \tag{3.25a}$$

for the accumulation-depletion case, and in a similar way (3.24c) leads to

$$J^h \cong \pm \nu^e \rho_s^e \left[1+\frac{\rho_1^h}{\rho_0^h}\right]\left[A_s^s \ln\left[1+\frac{\rho_1^h}{\rho_0^h}\right]+A_4 \ln^2\left[1+\frac{\rho_1^h}{\rho_0^h}\right]+\cdots\right] \tag{3.25b}$$

for the inversion case. Equations (3.25) are, of course, invalid (at some surface potentials φ_{0s}, at least) if ρ_1^h/ρ_0^h at $|x|=h-L$ is too large or if ν^e and ν^h, the receptivities of the surface to electrons and holes, are very different. When (3.25a) and (3.25b) are applicable, the current density at the surface is seen to depend on either one "receptivity" of the interface to the surface minority carrier (ν^e or ν^h) or the other, but not on both.

From (3.24) we can also deduce the small-signal forms of the outer conditions. By invoking the assumption $\rho_1^h \ll \rho_0^h$ at $|x|=h-L$, it is easily seen that the three forms of (3.24) coalesce into the single form of the Shockley condition (3.15) with

$$s=\frac{A_s^s}{\rho_b^h}\frac{1}{(1/\nu^e\rho_s^e)-1/\nu^h\rho_s^h}, \tag{3.26}$$

where ρ_b^h (the bulk value)$\equiv\rho_0^h(|x|=h-L)$. Thus under well-defined restrictions, i.e., small-signal conditions, $L \ll h$, and negligible right-hand sides of (3.23), the conditions used in the conventional approach to the steady-state photoconductivity experiment are, in fact, in accordance with the asymptotic limit of the consistent description employed here. The above derivation answers all macroscopic questions posed earlier on the meaning, justification, and limitations of the surface-recombination velocity condition (3.15) as applied to this dc case. In particular, we note that even when a condition such as (3.15) is applicable, the quantity s is not simply characteristic of the interface but depends also on the bulk constant ρ_b^h and on elements of the static solution, which are in turn dependent on surface and bulk constants, insulator properties, and the applied bias.

As stated previously, in the fully macroscopic approach presented here the complete description of the semiconductor interface is provided by measuring the various material surface coefficients appearing in the semiconduction boundary conditions. Since we have shown that the surface-recombination velocity condition is valid in some instances, it may be possible to determine some coefficients appearing in (3.26) by using measurements of s given in the literature. On account of inaccuracies in the analysis of the steady-state experiment (especially in the value of G) these s values are typically found using transient methods. From the above treatment it can be concluded that "outer"-condition-type approaches, such as the Shockley technique, are not valid for transient situations. However, if one restricts attention to the "tail" of the decay—as is always done[31]—then a quasi-dc analysis using "outer" conditions can be justified.[32] Moreover, transient procedures can ensure satisfaction of small-signal restrictions on the surface-recombination velocity condition, since measured values of s at a given bias will be nonconstant until the small-signal regime is reached. At this point it should be emphasized that with the two semiconduction boundary conditions (3.7) and (3.8) there is no need to ignore the initial rapid decay. The appropriate initial-value problem can be solved, and a description of the *full* transient can be obtained and used for the determination of surface coefficients.

All detailed surface-recombination velocity studies in the literature, to our knowledge, are for germanium, while all our analyses and calculations in Ref. 1 and Sec. IV of this paper are for silicon. Nevertheless, we feel it is of interest to calculate surface-recombination velocities using material surface coefficients obtained from measurements on Si-SiO_2 interfaces and to compare the results with published data for germanium. The surface-recombination velocity versus static surface potential φ_{0s} for a germanium sample determined from transient measurements is given in Ref. 33 and reproduced in Fig. 3. First we note that (3.26) clearly shows s to be positive, since A^s is generally found to be negative, and thermodynamic arguments given in Appendix A constrain $\nu^e>0$ and $\nu^h>0$. In Fig. 4 we plot the logarithm of (3.26) using data from silicon samples and assuming that ν^e, ν^h, and A^s are independent of the static solution, i.e., of φ_{0s}, along with the natural logarithm of the measured values of s for the germanium sample plotted in Fig. 3. It can be seen from the figure that the curves have the same shape, but that the experimental curve is much wider than the calculated curve. The lack of quantitative agreement is, of course, not surprising, since the calculations are for one material and the measurements are for another.

We now proceed with some detailed calculations

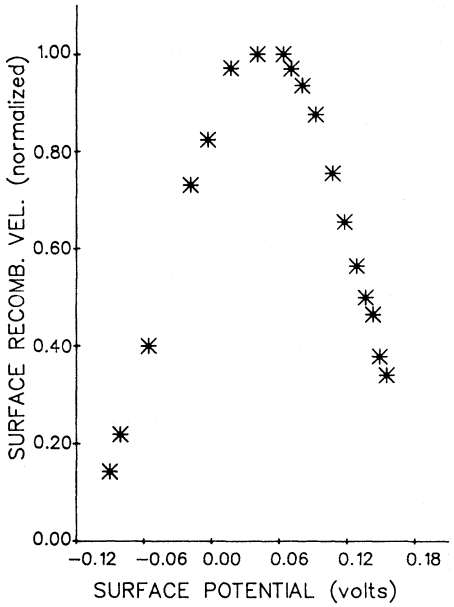

FIG. 3. Surface-recombination velocity plot from Many and Gerlich, Ref. 33.

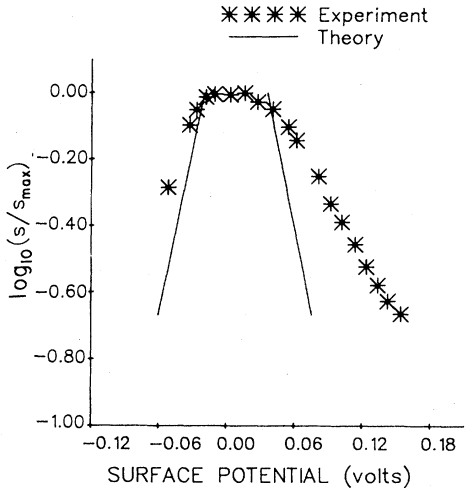

FIG. 4. Comparison of theoretical and experimental surface-recombination velocity curves on a semilogarithmic plot. Data from Ref. 33.

for silicon for which more extensive data for the determination of the material surface coefficients are available. To represent the Si-SiO_2 interface we employ the surface-force constitutive expressions given in (2.19) and (2.20). Work in Ref. 1 and in Sec. IV of this paper suggests that these forms are reasonable for Si-SiO_2 interfaces. However, it should be noted that no conclusive demonstration of the validity of the forms chosen is given either in Ref. 1 or in this paper and that, consequently, neither the forms nor the coefficient values should be regarded as definitive.

The material surface coefficients needed to describe dc situations have been determined using the methods of Ref. 1 and of Sec. IV of this paper. It turns out that reasonable accuracy is obtainable assuming the material surface coefficients A_i vanish for $i > 5$. These coefficients along with other material and geometric constants for several samples are shown in Table I with the literature sources cited. For sample 2 two sets of surface coefficients have been calculated under the assumptions that either the dopant concentration is uniform over the sample or it has been redistributed during the

TABLE I. Geometric and material constants for several samples.

Source type	Sample 1 Ref. 11, Figs. 14 and 25 n	Sample 2 Ref. 11, Fig. 14 Uniform P	Sample 2 Ref. 11, Fig. 14 Redistributed[a]	Sample 3 Ref. 45, Sample 6A1 n
Dopant (bulk) concentration (cm^{-3})	1.15×10^{16}	2.08×10^{16}	2.08×10^{16}	4.2×10^{14}
h (cm)	10^{-3}	10^{-3}	10^{-3}	10^{-3} (assumed)
l (cm)	6.8×10^{-6}	5.4×10^{-6}	5.4×10^{-6}	10^{-5}
a (cm^2)	1.1×10^{-3}	1.1×10^{-2}	1.1×10^{-2}	4.6×10^{-3}
A_1 (cm)	-1.8×10^{-5} (assumed)	-1.8×10^{-5}	-1.8×10^{-5}	-4.7×10^{-5}
A_2 (cm)	6.3×10^{-5}	7.3×10^{-5}	7.1×10^{-5}	1×10^{-4}
A_3 (V)	1.1×10^{-2}	-5×10^{-2}	-7.3×10^{-2}	-3.8×10^{-2}
A_4 (V)	-1.2×10^{-3}	5.6×10^{-3}	6.2×10^{-3}	-4.6×10^{-3}
A_5 (V)	-9.7×10^{-5}	-1.4×10^{-4}	-1.4×10^{-4}	-2.2×10^{-4}
v^h (n type) or v^e (p type) for depletion (cm/V sec)	6.7×10^{2}	5.2×10^{3}	5.2×10^{3}	

[a]An impurity profile $\rho^i=\rho_s^i e^{-x/d}$ with $\rho_s^i=-5\times10^{-4}$ C/cm^2 and $d=1.7\times10^{-5}$ cm has been assumed. This approximates findings of Grove (Ref. 25) for B in Si.

growth of the thermal oxide layer. This redistribution is a well-known phenomenon[34] (notably occurring with boron in the Si-SiO_2 system as in sample 2) that alters the dopant concentration adjacent to the interface and can thereby strongly affect the surface electric field in the semiconductor, and as a result it can have a significant influence on the A_i coefficients. Consequently, if the assumed dopant redistribution for sample 2 is realistic and if the choices for surface-force constitutive expressions (2.19) and (2.20) are reasonable, then the surface coefficients found for the redistributed case are truly characteristic of the interface, while those obtained assuming uniform dopant concentration ascribe to the surface properties that, in actuality, are of bulk origin.[35]

In making use of the surface coefficient values of Table I, a perhaps obvious but very important point of the fully macroscopic approach employed in this paper should be noted. This is that if (2.19) and (2.20) are in fact good choices for f^e and f^h, the surface coefficients of Table I, which have been determined from MOS capacitor studies, must be the same as those that would be found by conducting a surface-recombination test on an identically processed sample because they are *material* coefficients. Analogously, any predictions concerning the behavior of a semiconductor layer in a steady-state photoconductivity experiment using the constants determined from MOS capacitor experiments must also be correct. To illustrate this point, in Fig. 5 we exhibit the surface-recombination velocity versus the surface potential that would be determined by a small-signal surface-recombination experiment on sample 1 of Table I. For this plot we have assumed that the ν^h value obtained from MOS admittance data in Sec. IV for sample 2, which is a *p*-type sample, is also valid for sample 1, which is a similarly processed *n-type* sample. In passing we note that the calculated values of s shown in Fig. 5 are much larger than those generally believed to be obtained for Si-SiO_2 interfaces.[34] This result indicates that the ν^e and ν^h values found in Sec. IV are probably incorrect and/or that the ν^h value used is not apropos for the *n*-type sample 1. This disagreement could also be evidence that the forms in (2.19) and (2.20) are invalid for Si-SiO_2 interfaces. In any case, we continue under the presumption that the above point, i.e., that (2.19) and (2.20) are "good" constitutive selections, has been verified.

The next illustration concerns the differences between the "outer" conditions for the low-level injection [Eqs. (3.24)] and small-signal cases [Eq. (3.15) with (3.26)]. In particular, we exhibit the error made when the conventional Shockley approach is used in analyzing a low-level injection situation. We

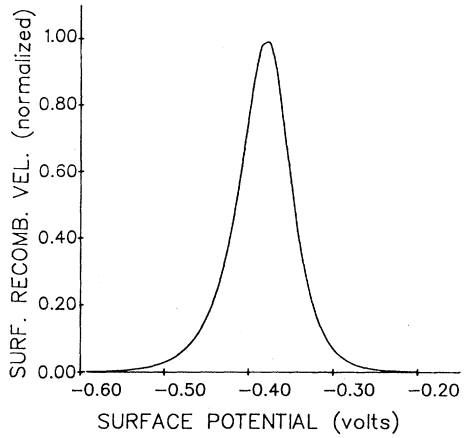

FIG. 5. Surface-recombination velocity (normalized) vs surface potential calculated using Eq. (3.26) and the constants for sample 1 of Table I with $s_{max}=1.1\times10^7$ cm/sec.

examine the steady-state photoconductivity experiment in which a low-level situation has been produced by making the charge-carrier source density due to photogeneration G fairly large. Figure 6 compares the added-charge-carrier density profile for sample 1 of Table I obtained when the appropriate low-level injection condition (3.24) is employed with that found using the surface-recombination velocity condition (3.15). The striking differences result from the fact that the interface absorbs carriers more efficiently than predicted by the surface-recombination velocity condition (3.15) as ρ_1^h in-

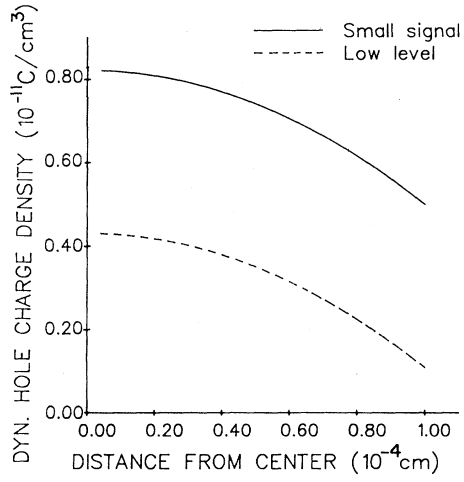

FIG. 6. Dynamic hole fluid charge-density profiles $\rho_1^h(x)$ calculated for sample 1 of Table I for low-level injection using either the small-signal expression (3.15) with (3.16) or the appropriate low-level expression (3.24). $\varphi_s=-0.2$ (depletion), $G=10^{-2}$ C/cm^3 sec, and the Debye layer thickness has been neglected.

creases and moves out of the small-signal range.[36]

In Fig. 7 we show the influence of the same error shown in Figure 6 on an s-vs-φ_s curve. The solid curve is obtained from (3.26) and shows the s that would be determined from a genuinely small-signal experiment (achieved, say, by lowering G). This s is a function only of the static solution. The dotted curve in Fig. 7 is for the assumed higher value of G and has been obtained by writing the "outer" condition in (3.24) in the form

$$J^h = \pm \hat{s} \rho_1^h \text{ at } |x| = h - L \ , \tag{3.27}$$

where $\hat{s}$ depends on ρ_1^h as well as on the static solution. The horizontal portion of the dotted curve was not calculated because that part of the curve is in a high-level regime and can be calculated only by solving the full set of equations (3.1)—(3.6) in the space-charge region subject to the full set of boundary conditions (3.7)—(3.11). The figure clearly shows the results to be quite different; that is, for a given surface the s values should change with the level of bulk illumination (G). Unfortunately, the literature on surface-recombination experiments in circumstances of low-level injection is very limited, and, to our knowledge, the widening effect predicted in Fig. 7 has never been observed experimentally.[37]

The final calculation of this section concerns the influence of redistributed dopant. As noted previously, dopant-redistribution effects are manifested through the electric field at the semiconductor surface. Thus, if $A_2 \simeq \epsilon_{\text{sem}} A_1 / \epsilon_{\text{ox}}$ [that is, if the B_1 term in (2.41) is negligible] then dynamic characteristics should not be affected by redistribution. This may be important because as seen in Ref. 1 static experiments do not definitively establish the necessity of a non-negligible B_1 but only suggest its plausibility. We have, as mentioned earlier, used the methods of Ref. 1 to determine the B_i coefficients ($B_1 \neq 0$) for sample 2 in Table II from which the A_i coefficients shown have been obtained. Based on these and on the values for ν^e and ν^h from sample 1 in Sec. IV we plot the predicted surface-recombination velocities in Fig. 8 for the uniform and redistributed cases. The significant differences between the two curves indicate the sizable errors that can be made in the description of the surface if the interior of the semiconductor is not described properly. Moreover, this calculation exhibits the preciseness with which semiconductor surfaces and their interaction with the interior may be discussed within the fully macroscopic theory. We again note that if the B_1 (field) term is negliglble, then the differences seen in Fig. 8 are not realistic.

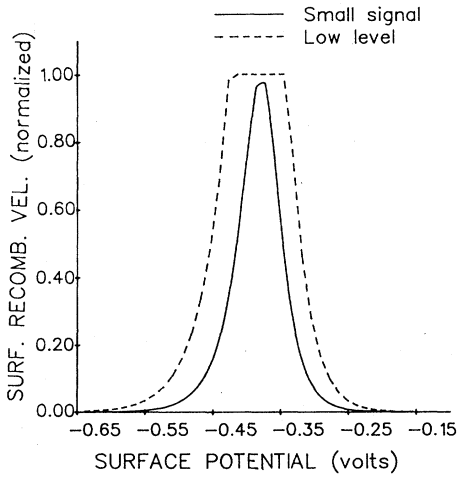

FIG. 7. Predicted surface-recombination velocities at two injection levels. The central horizontal portion of the dashed curve is in a high-level regime, which we have not treated. Parameters are as given in Fig. 6.

IV. APPLICATION TO THE Si-SiO$_2$ INTERFACE UNDER SMALL-SIGNAL ac CONDITIONS

Many analyses of the familiar MOS admittance experiment have appeared in the literature,[38] but as indicated in the Introduction, to our knowledge no field-theoretic description of the experiment has ever been given. Such an analysis is presented in this section. As there are no existing purely continuum approaches and no accepted boundary conditions for such a treatment, we do not engage in any detailed comparisons with past work. The conventional description, consisting of equivalent circuits coupled with the Shockley-Read-Hall model, will not be discussed in depth because not being a field theory, it does not contain partial-differential equations and the associated consistent boundary conditions that

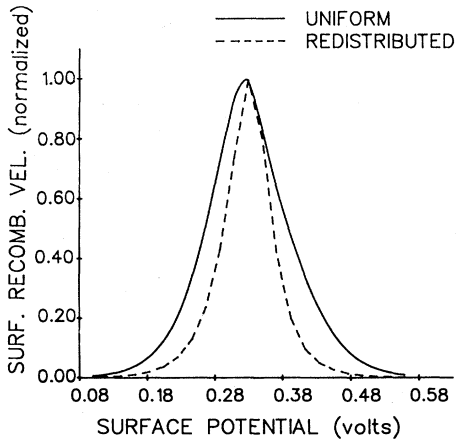

FIG. 8. Comparison of two theoretical curves obtained from (3.15) assuming either uniform or redistributed dopant for sample 2 of Table I.

enable a unified macroscopic approach to *all* semiconductor interface situations, but rather provides a quasimicroscopic procedure for obtaining equivalent circuit parameters associated with interfaces for use in the small-signal description only. Nonetheless, as noted in the Introduction, because we treat the small-signal (linear) situation our admittance expressions derived from the field theory will appear similar to comparable equivalent circuit expressions. If desired, one could, in fact, deduce the equivalent circuits corresponding to our results and thereby enable a detailed comparison with previous work. This, and the experimental support for any difference, will be left to future investigation. Here, we wish simply to note that equivalent circuit models connected directly to the underlying macroscopic physics may be derived in this manner and in so doing one can avoid the art normally involved in constructing such models. In any case, as has previously been stated, our chief interest in the present work is in the exposition and illustration of the fully macroscopic approach to interface description. Of most importance in the applications is showing the capability of describing standard experiments and not in detailed quantitative agreement with observation.

As in the previous applications in Sec. III of this work and in Ref. 1, the field theory is implemented by formulating and solving (approximately) a relevant boundary-value problem. For the MOS admittance experiment this proceeds as follows. A schematic diagram of the experimental configuration is shown in Fig. 9. The semiconductor portion of the structure consists of an epilayer of thickness h grown on a high-conductivity substrate. Interposed between the epilayer and the metal (gate) contact is an insulating oxide layer of thickness l. A static biasing voltage $\bar{\varphi}_0$ and an ac excitation signal $\bar{\varphi}_1 e^{i\omega_0 t}$ are applied at the gate, and the total current is measured. In formulating the boundary-value problem

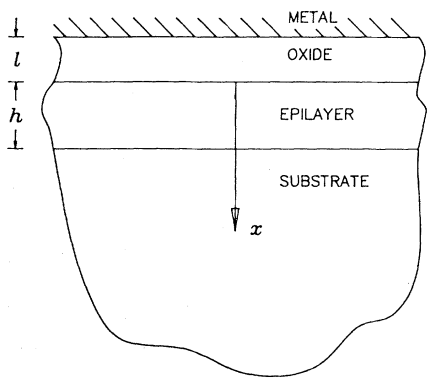

FIG. 9. Schematic diagram of the structure used in the MOS admittance experiment.

associated with this experiment we assume that the one-dimensional,[39] small-signal[40] forms of the governing equations discussed in Sec. II are applicable. Since for the ac situation, the semiconduction boundary conditions (2.39) and (2.40) require (to be shown in this section) dissipative terms that take the form of convolution integrals in time, it is helpful to take the Fourier transform of all the equations. Hence, if we define

$$r(\omega,x)\equiv\mathcal{F}\{r(t,x)\}\equiv\int_{-\infty}^{\infty} r(t,x)e^{-i\omega t}dt\ , \quad (4.1)$$

where r is any of ρ_1^e, ρ_1^h, J^e, J^h, or φ_1, and make use of

$$\mathcal{F}\left\{\frac{\partial r^m(t,x)}{\partial t^m}\right\}=(i\omega)^m r(\omega,x) \quad (4.2)$$

and

$$\mathcal{F}\left\{\int_{-\infty}^{\infty} r_1(s,x)r_2(t-s,x)ds\right\}=r_1(\omega,x)r_2(\omega,x)\ , \quad (4.3)$$

then from (2.24)–(2.29) the differential equations in the transformed small field variables take the form

$$J^e=\mu^e\rho_1^e\frac{d\varphi_0}{dx}+\mu^e\rho_0^e\frac{d\varphi_1}{dx}-D^e\frac{d\rho_1^e}{dx}\ , \quad 0\le x\le h \quad (4.4)$$

$$J^h=-\mu^h\rho_1^h\frac{d\varphi_0}{dx}-\mu^h\rho_0^h\frac{d\varphi_1}{dx}-D^h\frac{d\rho_1^h}{dx}, \quad 0\le x\le h \quad (4.5)$$

$$i\omega\rho_1^e+\frac{dJ^e}{dx}=-\gamma^h, \quad 0\le x\le h\ , \quad (4.6)$$

$$i\omega\rho_1^h+\frac{dJ^h}{dx}=\gamma^h, \quad 0\le x\le h \quad (4.7)$$

$$\frac{d^2\varphi_1}{dx^2}=-\frac{1}{\epsilon_{\rm sem}}(\rho_1^e+\rho_1^h), \quad 0\le x\le h \quad (4.8)$$

$$\frac{d^2\varphi_1}{dx^2}=0 \ \text{(oxide)}, \quad -l\le x\le 0 \quad (4.9)$$

and we note that appropriate expressions for γ^h in (4.6) and (4.7) will be selected later. From (2.36)–(2.40) the transformed small-signal boundary conditions take the form

$$\varphi_1=2\pi\bar{\varphi}_1\delta(\omega-\omega_0) \ \text{ at } x=-l \quad (4.10)$$

$$-i\omega\epsilon_{\rm ox}\frac{d\varphi_1}{dx}=2\pi J_m\delta(\omega-\omega_0) \ \text{ at } x=-l \quad (4.11)$$

$$\varphi_1\,|_{\rm ox}=\varphi_1\,|_{\rm sem} \ \text{ at } x=0 \quad (4.12)$$

$$J^e+J^h-i\omega\epsilon_{\text{sem}}\left.\frac{d\varphi_1}{dx}\right|_{\text{sem}} = -i\omega\epsilon_{\text{ox}}\left.\frac{d\varphi_1}{dx}\right|_{\text{ox}} \quad \text{at } x=0 \tag{4.13}$$

$$A_1\left.\frac{d\varphi_1}{dx}\right|_{\text{ox}}+A_2\left.\frac{d\varphi_1}{dx}\right|_{\text{sem}} + \frac{\rho_1^e}{\rho_0^e}A_e-\frac{J^e}{\nu^e\rho_0^e}=0 \quad \text{at } x=0 \tag{4.14}$$

$$A_1\left.\frac{d\varphi_1}{dx}\right|_{\text{ox}}+A_2\left.\frac{d\varphi_1}{dx}\right|_{\text{sem}} - \frac{\rho_1^h}{\rho_0^h}A_h+\frac{J^h}{\nu^h\rho_0^h}=0 \quad \text{at } x=0 \tag{4.15}$$

$$\varphi_1=\rho_1^e=\rho_1^h=0 \quad \text{at } x=h\ , \tag{4.16}$$

$$J^e+J^h-i\omega\epsilon_{\text{sem}}\frac{d\varphi_1}{dx}=2\pi J_m\delta(\omega-\omega_0) \quad \text{at } x=h \tag{4.17}$$

where

$$A_e\equiv A^s+i\omega E(\omega)\rho_0^e,$$

$$A_h\equiv A^s-i\omega H(\omega)\rho_0^h\ ,$$

$$\begin{Bmatrix}E(\omega)\\H(\omega)\end{Bmatrix}=\int_{-\infty}^{\infty}\begin{Bmatrix}E(t)\\H(t)\end{Bmatrix}\times e^{-i\omega t}dt\ ,$$

$J_m\equiv I/a$, where I is the current through the gate electrode and a is the gate contact area, and we have assumed standard Ohmic contact conditions at $x=h$ [Eq. (4.16)] since the substrate is highly conducting. Also, in deriving (4.14) and (4.15) from (2.39) and (2.40) $E(t)$ and $H(t)$ have been taken to vanish for negative arguments (causality).[41] Equations (4.4)–(4.17) constitute the complete specification of the transformed MOS admittance problem within the framework of the fully macroscopic description of bounded semiconductors. When the solution of the transformed problem has been found, the solution to the original problem is obtained from the inverse transform in the usual manner, i.e.,

$$r(t,x)\equiv\mathcal{F}^{-1}\{r(\omega,x)\} \equiv\frac{1}{2\pi}\int_{-\infty}^{\infty}r(\omega,x)e^{i\omega t}d\omega\ . \tag{4.18}$$

The solution of the problem specified in (4.4)–(4.17) is facilitated by first reducing it to a boundary-value problem in the epilayer region alone. To this end we integrate (4.9) and employ the conditions (4.10) and (4.11) to obtain

$$\varphi_1(\omega,x)=\left[\frac{J_m i}{\omega\epsilon_{\text{ox}}}(x+l)+\bar{\varphi}_1\right]2\pi\delta(\omega-\omega_0), \quad -l\le x\le 0 \tag{4.19}$$

in the oxide layer. Equations (4.12) and (4.13) along with (4.19) and its first derivative, respectively, evaluated at $x=0^-$ then yield

$$\varphi_1=\left[\frac{J_m il}{\omega\epsilon_{\text{ox}}}+\bar{\varphi}_1\right]2\pi\delta(\omega-\omega_0) \quad \text{at } x=0^+\ , \tag{4.20}$$

$$J^e+J^h-i\omega\epsilon_{\text{sem}}\frac{d\varphi_1}{dx}=2\pi J_m\delta(\omega-\omega_0) \quad \text{at } x=0^+\ . \tag{4.21}$$

Finally, substituting from (4.19) for $d\varphi_1/dx\,|_{\text{ox}}$ into (4.14) and (4.15) we find

$$\frac{2\pi i A_1 J_m\delta(\omega-\omega_0)}{\omega\epsilon_{\text{ox}}}+A_2\left.\frac{d\varphi_1}{dx}\right|_{\text{sem}}+\frac{\rho_1^e}{\rho_0^e}A_e - \frac{J^e}{\nu^e\rho_0^e}=0 \quad \text{at } x=0^+ \tag{4.22}$$

$$\frac{2\pi i A_1 J_m\delta(\omega-\omega_0)}{\omega\epsilon_{\text{ox}}}+A_2\left.\frac{d\varphi_1}{dx}\right|_{\text{sem}}-\frac{\rho_1^h}{\rho_0^h}A_h + \frac{J^h}{\nu^h\rho_0^h}=0 \quad \text{at } x=0^+\ . \tag{4.23}$$

The four boundary conditions (4.20)–(4.23) with the differential equations (4.4)–(4.8) and the additional boundary conditions in (4.16) comprise the aforementioned problem for the epilayer region. Since more than one of (4.20)–(4.23) contains the complex constant J_m, which is often unknown, it is helpful to change variables by incorporating $2\pi J_m\delta(\omega-\omega_0)$ into the dynamic field variables. In this way J_m is eliminated from all equations except (4.20). The epilayer problem consisting of the boundary conditions (4.16) and (4.21)–(4.23) and the differential equations (4.4)–(4.8) [all divided by $2\pi J_m\delta(\omega-\omega_0)$] may now be solved directly, after which the condition (4.20) serves either to calculate J_m given $\bar{\varphi}_1$ or given both J_m (from admittance data) and $\bar{\varphi}_1$ to determine unknown dissipative material surface coefficients. Denoting the quantities divided by $2\pi J_m\delta(\omega-\omega_0)$ with carets, we observe using (4.18) that

$$\frac{\varphi_1(x,t)}{J_m}=\int_{-\infty}^{\infty}\hat{\varphi}_1(x,\omega)\delta(\omega-\omega_0)e^{i\omega t}d\omega =\hat{\varphi}_1(x,\omega_0)e^{i\omega_0 t} \tag{4.24}$$

and consequently from (4.20), since $J_m=I/a$, that

$$Y(\omega_0)\equiv G_p(\omega_0)+iS_p(\omega_0)=\frac{a}{\hat{\varphi}_1(0,\omega_0)}\ , \qquad (4.25)$$

where Y, G_p, and S_p are the admittance, conductance, and susceptance of the MOS capacitor with the impedance due to the oxide subtracted off, following Ref. 11. Since in this section (and in Appendix B) we are interested solely in calculating Y, by virtue of (4.25) we need work only with the transformed small-field variables divided by $2\pi J_m\delta(\omega-\omega_0)$, which are henceforth shown without carets.

As noted in the Introduction asymptotic "outer"-condition-type approaches like that of Sec. III are not applicable to the problem posed in this section. There are several reasons for this, connected both with the ability to derive an "outer" condition and with the need to deduce a value for φ at the interface after having solved the "outer" problem. The primary difficulties are associated with nonconstancy of the carrier currents across the space-charge layer (because of depletion-layer generation) and with the presence of the electric field and charge-rate terms [$E(\omega)$ and $H(\omega)$] in (4.22) and (4.23). Consequently, a solution to the full boundary-value problem formulated above, including the portion in the space-charge region, must be pursued.

This problem can be solved only numerically (except when $\varphi_s=0$) because of the nonconstant coefficients in the differential equations (4.4) and (4.5). However, since our intent is solely to illustrate method, highlighting the role of the semiconduction boundary conditions, a full numerical calculation is unnecessary and perhaps even misleading. Instead, approximate analytical derivations for the important cases of depletion and inversion are undertaken. Owing to their length these are given in Appendix B; in this section we simply state and discuss the results. Initially, we set the charge-rate terms $E(\omega)$ and $H(\omega)$ to zero and thereby obtain predictions of ac behavior based on a theory that describes static and dc situations. Subsequently, comparison with experiment will demonstrate why and in what circumstances these terms are required.

For the case of depletion the admittance calculated in Appendix B is given by (B12). For convenience we rewrite this in terms of the auxiliary B_i coefficients defined at the end of Sec. II and find

$$Y(\omega_0)\cong a\omega_0\left[-(B_1+\epsilon_{\rm sem})\frac{d}{d\varphi_s}\left[\frac{d\varphi_0}{dx}\bigg|_{\rm sem}\right]+\frac{B^s\beta^e\rho_s^e}{\omega_D}+\frac{i\omega_0\epsilon_{\rm sem}}{\omega_D L}\right]\left[\frac{i+\omega_0/\omega_D}{1+\omega_0^2/\omega_D^2}\right], \qquad (4.26a)$$

$$\omega_D\equiv-\beta^e\rho_s^e+\left[\frac{1}{\beta^h\rho_s^h}-\frac{B^sL_p}{\mu^h\rho_b^h}\tanh\frac{h}{L_p}\right]^{-1}, \qquad (4.26b)$$

where $B^s\equiv-\mu^eA^s\epsilon_{\rm ins}/D^eA_1$, $E(\omega)$ and $H(\omega)$ have been set to zero, ρ_s^e is the static electron charge density at the interface, and the derivation restricts $\bar{\varphi}_s\le-3$. The quantity L_p [$\equiv(D^h\tau_p)^{1/2}$] is the bulk diffusion length for holes, a is the gate area, and L is the depletion-layer width. Surface effects enter this solution through the surface coefficients appearing in (4.26); namely, through B^s and B_1 (or A_1, A_2, and A^s), which characterize the static surface response to electric field and carrier density (potential), respectively, and through β^e and β^h (or ν^e and ν^h), which quantify dependences on the electron and hole fluid velocities at the interface. These latter terms may be viewed as surface mobilities or "receptivities," which, as discussed in Appendix A, account for energy dissipation as the charged fluids are slowed from their nonzero macroscopic velocities in the interior to zero velocity at the interface. As will be seen, in the interpretation of experiment the surface receptivities play much the same role as the conventional "interface trap capture cross sections."

In deriving an analogous expression valid for inversion it is essential that the important effects of carrier generation in the depletion layer be incorporated. To do this we specify γ^h in (4.6) and (4.7) to be

$$\gamma^h=\frac{\rho_1^e-\rho_1^h}{\tau},\quad L_s<x<L \qquad (4.27)$$

where L_s and $L-L_s$ are the approximate thicknesses of the inversion layer and the depletion layer, respectively, and τ is a "lifetime" (a bulk material constant) characteristic of the generation-recombination processes. The approximate admittance expression obtained in Appendix B is given in (B23) and reproduced below [again setting $E(\omega_0)=H(\omega_0)=0$ and recasting in terms of the auxiliary B_i coefficients]:

$$Y(\omega_0)\cong a\omega_0\left[-(B_1+\epsilon_{\rm sem})\frac{d}{d\varphi_s}\left[\frac{d\varphi_0}{dx}\bigg|_{\rm sem}\right]+\frac{\Delta}{\omega_I}+\frac{i\omega_0\epsilon_{\rm sem}}{\omega_I L_d}\right]\left[\frac{i+\omega_0/\omega_I}{1+\omega_0^2/\omega_I^2}\right], \qquad (4.28a)$$

$$\omega_I \equiv -\beta^e \rho_s^e + \left[\frac{1}{\beta^h \rho_s^h} - \frac{B^s}{\Delta} \right]^{-1} , \tag{4.28b}$$

where

$$\Delta \equiv \frac{\mu^h \rho_b^h}{L_p} \coth \frac{h}{L_p} - \frac{L_d \rho_b^h}{\varphi_d \tau} \exp(\mu^h \varphi_d / D^h) .$$

The quantity ρ_s^h is the static hole charge density at the surface, φ_d is the static potential drop across the depletion layer of thickness L_d ($\equiv L - L_s$), and, as before, L_p is the bulk diffusion length for holes. We note that φ_d and L_d, which arise from approximations made in Appendix B, are not precisely defined quantities. As in (4.26), all effects of the interface on the inversion admittance are expressed by the appearance of various coefficients in (4.28).

We now discuss the above admittance expressions—predictions of a description developed from static and dc observations—in greater detail beginning with the depletion result of (4.26). The frequency given in (4.26b) characterizes the semiconductor-interface response in depletion. The first term in (4.26b) clearly represents the contribution arising from the interaction of the electron gas with the surface, while the second describes a similar interaction of the hole gas modified by the restrictions imposed on the hole supply by diffusion from the bulk. The first term generally dominates the second [unless the receptivity of the interface for electrons and holes is very different, i.e., $\beta^h \gg \beta^e$, $L_p \tanh(h/L_p)/\mu^h \rho_b^h$ large] so that ω_D may be approximated by

$$\omega_D \cong \omega_e \equiv -\beta^e \rho_s^e , \tag{4.29}$$

where ω_e is a frequency associated with the response of the surface to electron gas alone. Inserting (4.29) into (4.26a) we find[42]

$$Y(\omega_0) \simeq -a\omega_0 \left[(B_1 + \epsilon_{\text{sem}}) \frac{d}{d\varphi_s} \left[\frac{d\varphi_0}{dx} \bigg|_{\text{sem}} \right] + B^s - \frac{i\omega_0 \epsilon_{\text{sem}}}{\omega_e L} \right] \left[\frac{i + \omega_0/\omega_e}{1 + \omega_0^2/\omega_e^2} \right] , \tag{4.30}$$

which with (2.41) and (B2) yields

$$Y(\omega_0) \cong -a\omega_0 \frac{d\sigma_0}{d\varphi_s} \left[\frac{i + \omega_0/\omega_e}{1 + \omega_0^2/\omega_e^2} \right] + \frac{ia\omega_0 \epsilon_{\text{sem}}}{L} , \tag{4.31}$$

where σ_0 is the static surface-charge density at the Si-SiO_2 interface. Equation (4.31) shows the amplitude of the admittance, e.g., the height of the conductance peak, to be governed by a combination of $ia\omega_0 \epsilon_{\text{sem}}/L$ and $d\sigma_0/d\varphi_s$. These are capacitances, the former being the familiar depletion-layer capacitance [which as seen from the derivation of (4.31) is the sum of space-charge capacitance and a capacitance originating from displacement current across the depletion layer], while the latter is an interface capacitance usually termed the "interface state density," $-qN_{ss}$.

The expressions for the admittance in (4.31) and for the response frequency in (4.29) are in conformity with conventional understanding when surface-potential fluctuations are not included.[38] Thus our direct derivation from the underlying macroscopic principles confirms the usual (equivalent circuit) results. The only difference is conceptual, with our expressions being couched in terms of macroscopic material coefficients rather than the quasimicroscopic quantities that characterize the "interface traps" in the Shockley-Read-Hall model. [The aforementioned similarity between our macroscopic surface receptivity and the quasimicroscopic capture cross section is evident from (4.29).] It will be noted that when the assumptions used to derive (4.31) and (4.29) are not valid, other expressions result, which we do not discuss.

As with the analogous conventional expressions the above equations predict "single-time-constant" behavior with the time constant $1/\omega_e$ being set by interface response to majority carriers (electrons). This, however, is known not to describe the depletion characteristics of a MOS capacitor wherein "frequency dispersion" is observed to occur. Conventionally, such behavior is explained by the reasonable quasimicroscopic surface-potential fluctuation model.[38] For a purely macroscopic theory, however, we require a more general description that is free of microscopic considerations.[43] In particular, such frequency dispersion indicates, in macroscopic terms, that a generalized "memory" or "relaxation" phenomenon is occurring. The standard macroscopic procedure[44] for handling this, e.g., in dielectric relaxation or viscoelasticity, is to include in the appropriate constitutive equations—here, the expressions for the surface forces f^e and f^h—linear functionals (integrals) of the histories of dependent variables. We emphasize that such a general treatment does not deny and could in fact incorporate the conventional description. Now, the thermodynamics presented in Appendix A suggests that the memory integrals for the surface forces be over the charge-rate histories, i.e., the histories of the time rates of change of the carrier densities at the interface. These were the convolution integrals that appeared in the surface-force expressions (2.19) and (2.20) and gave rise to the $E(\omega)$ and $H(\omega)$ functions in (4.14) and (4.15). Again, these terms are required

to explain the frequency dispersion observed in the depletion characteristics of MOS capacitors.

That the terms $E(\omega)$ and $H(\omega)$, which describe the frequency dispersion, arise from rate effects leads one to expect that at lower frequencies these terms should be negligible and (4.31) and (4.29) applicable. The experimental evidence supports this expectation: Saks[45] employed formulas identical to (4.31) together with admittance measurements in depletion at a constant low frequency ($\sim 1-10$ Hz) to obtain N_{ss} ($\equiv -d\sigma_0/qd\varphi_s$) values in excellent agreement with quasistatic determinations.

The admittance expressions analogous to (4.31) and (4.29) that incorporate the charge-rate effects are shown below (see Appendix B for derivation):

$$Y(\omega_0 \cong -a\omega_0 \left[\frac{d\sigma_0}{d\varphi_s} + i\omega_0 e(\omega_0) \right] \times \left[\frac{i+\omega_0/\omega_D}{1+\omega_0^2/\omega_D^2} \right] + \frac{i\omega_0 a \epsilon_{\text{sem}}}{L} , \quad (4.32a)$$

$$\omega_D = -\beta^e \rho_s^e . \quad (4.32b)$$

Since the charge-rate term $e(\omega)$ appears only in (4.32a), these equations suggest that to first order the amplitude of the admittance [Eq. (4.32a)], but *not* the interface response frequency [Eq. (4.32b)], will be dependent on the rate of change of the carrier densities at the interface. This is, in fact, in accord with experiment; as is well known, in a plot of the conductance G_p/ω vs ω the peak amplitude and the peak shape are affected by the dispersion, *but* the location of the peak and its variation with bias are unaffected and remain in agreement with (4.32b).[11] This result, which follows directly from our analysis, is not nearly as simply or clearly shown by conventional work.[11] Moreover, it supports our argument that it is the charge rates that are responsible for the "memory" effects observed. Finally, we note that (4.32a) indicates that, not surprisingly, it is the rate of change of the majority-carrier density (electrons) at the interface that is crucial.

In view of the foregoing, (4.32b) provides a ready means of determining the surface receptivity for electrons β^e (or ν^e) in depletion (for n-type material). This was the technique by which the values for ν^e and ν^h (for a p-type sample) given in Table I were found. (See Sec. III for some trial calculations made using these values.) Equation (4.32a) together with admittance data as a function of bias and frequency may equally readily be employed for determining the electron-rate term $e(\omega)$ [or $E(\omega)$] in depletion. This will not be undertaken here because the generality of the function $e(\omega)$ makes it capable of fitting any single experimental result, and thus such a determination would not provide any additional understanding. Further experimental work, e.g., a transient experiment, would be required to confirm the particular $e(\omega)$ found and thereby validate the overall picture presented. In any case, it is evident that the macroscopic treatment is indeed capable of describing the depletion behavior.

We next examine the inversion expression given in (4.28). The freqency ω_I (like ω_D in the depletion case) is characteristic of the semiconductor response in inversion and again shows the contributions from interface response to electrons ($-\beta^e\rho_s^e$) plus the response to holes ($\beta^h\rho_s^h$) as modified by hole diffusion from the bulk [$\mu^h\rho_b^h \coth(h/L_p)/L_p$] and also by depletion-layer generation of holes [$-L_d\rho_i^h \exp(\mu^h\varphi_d/D^h)/\varphi_d\tau$]. Contributing to the amplitude of the admittance, we see terms arising from space-charge capacitance [$\epsilon_{\text{sem}} d(d\varphi_0/dx \mid_{\text{sem}})/d\varphi_s$], a (new) capacitance associated with the static electric field coefficient B_1 [$B_1 d(d\varphi_0/dx \mid_{\text{sem}})/d\varphi_s$], a term resulting from the bulk generation-diffusion of holes (Δ/ω_I), and lastly, a term arising from displacement current across the depletion layer ($i\omega_0\epsilon_{\text{sem}}/\omega_I L_d$). Individually, all of these terms except the static electric field term are familiar.

Now, in the high-frequency limit ($\omega \gg \omega_I$) only the displacement-current contribution remains and, as it should, Y reduces to a susceptance corresponding to the usual depletion-layer capacitance. On the other hand, in the low-frequency limit ($\omega \ll \omega_I$), because $-\Delta/\beta^s$ is typically much greater than $-\beta^e\rho_s^e$ but much less than $\beta^h\rho_s^h$, we see that Y simplifies to a familiar sum of static capacitances (space charge plus interface). Thus, in both of these limiting cases, (4.28) reduces in agreement with well-known observations. At intermediate (but still low) frequencies it is equally well known that a plot of the conductance G_p/ω vs ω is of "single-time-constant" form with the peak occurring at a much lower frequency than that for the same sample in depletion.[11] Single-time-constant behavior is, of course, in agreement with (4.28) since the charge-rate terms $e(\omega)$ and $h(\omega)$ (which produce frequency dispersion) have been omitted from the derivation. The observed absence of frequency dispersion indicates that these terms are, in fact, negligible for the inversion case. Evidently the frequencies at which a conductance is observed (including the peak frequency ω_I) are sufficiently low that, as in the depletion case at low frequency, the ac behavior is set by the same coefficients as the dc behavior, i.e., the surface receptivity

β^e (or ν^e).

Because sufficiently detailed experimental evidence is not available from the literature concerning the inversion case we do not engage in a closer examination of the admittance given in (4.28). This must be left to future work. Nonetheless, it is evident that these equations incorporate all of the important physics of the inversion situation: majority- and minority-carrier interface response, minority-carrier charge capacitance, displacement current across the depletion layer, and static electric field effects. Moreover, from the above, it is seen that they do explain the main qualitative features from admittance observed in inversion. Finally, detailed quantitative agreement between theory [with perhaps some minor modifications to the constitutive choices for f^e and f^h given in (2.19) and (2.20)] and experiment should be obtainable.

Note added in proof. Experimental work by one of the authors (M.G.A.) has verified the necessity for the electric field terms in (4.14) and (4.15), i.e., the B_1 term in (2.41), in the case of weak inversion in a future publication [J. Appl. Phys. (in press)].

ACKNOWLEDGMENTS

This work was supported in part by the National Science Foundation under Grant No. ENG 7827637.

APPENDIX A: THERMODYNAMICS OF THE SEMICONDUCTOR-INSULATOR INTERFACE

In Ref. 1 (Appendix A) the first and second laws of thermodynamics for the infinite semiconducting continuum were derived, from which the required constitutive equations for the bulk were obtained. In this appendix the corresponding first and second laws of thermodynamics for the semiconductor-insulator interface are obtained and then used to develop the surface constitutive theory, in particular, finding the functional dependences for the surface forces f^e and f^h. It should be noted that this task is somewhat more complicated than the development of the volumetric constitutive theory, because whereas the material fields $\vec{E}^e$ and $\vec{E}^h$ are purely dissipative, their surface counterparts, i.e., the surface forces f^e and f^h, act both to store and dissipate energy. Further difficulties arise from the fact that it is impossible to decompose the surface forces into a simple sum of recoverable and dissipative parts.[46]

As usual, the requisite surface relations are deduced from volumetric expressions by taking limits of integral forms written for appropriate pillbox regions. For our purposes a convenient form of the volumetric equation of energy balance is Eq. (A5) of Ref. 1 integrated over an arbitrary fixed volume V, which enables us to write

$$\int_V \left[\frac{d\epsilon}{dt} + \left[\rho^e \frac{\partial \epsilon^e}{\partial T} + \rho^h \frac{\partial \epsilon^h}{\partial T} \right] \frac{\partial T}{\partial t} - \vec{E} \cdot \frac{d\vec{P}}{dt} + \rho^e \vec{E}^e_{rd} \cdot \vec{v}^e + \rho^e \vec{E}^e_d \cdot \vec{v}^e + \rho^h \vec{E}^h_d \cdot \vec{v}^h + \rho^h \vec{E}^h_{rd} \cdot \vec{v}^h + \gamma^e \varphi^e + \gamma^h \varphi^h - g \right] dV = 0 , \quad \text{(A1)}$$

where the constitutive relations derived in Ref. 1 for the fluid pressures p^e and p^h [(A13), Ref. 1] and the definitions of the chemical potentials φ^e and φ^h [(A14), Ref. 1] have been employed. The material fields $\vec{E}^e$ and $\vec{E}^h$ have been split into purely dissipative (subscript d) and mixed recoverable-dissipative (subscript rd) terms in preparation for the discussion that follows. (Note that except in the boundary surface limit only $\vec{E}^e_d$ and $\vec{E}^h_d$ are nonzero). Also, an energy source density g has been included to account for radiant energy absorption (emission) in cases involving photoexcitation (radiative recombination) of carriers. To derive a balance expression for surface energy from (A1) the volume V is taken to be a standard pillbox region that is bisected by a portion of the semiconductor-insulator interface. In the limit as the volumetric region collapses to the interface we allow ϵ, ρ^e, ρ^h, γ^e, γ^h, $\vec{n} \cdot \vec{E}^e_d$, $\vec{n} \cdot \vec{E}^e_{rd}$, $\vec{n} \cdot \vec{E}^h_d$, $\vec{n} \cdot \vec{E}^h_{rd}$ ($\vec{n}$ is the outwardly directed unit normal to the interface), and g to become unbounded in such a way that

$$\frac{d\epsilon}{dt} dV \to \frac{d\epsilon^s}{dt} dS , \quad \text{(A2)}$$

$$\rho^e \frac{\partial \epsilon^e}{\partial T} dV \to \sigma^e \frac{\partial \epsilon^e}{\partial T_s} dS ,$$

$$\rho^h \frac{\partial \epsilon^h}{\partial T} dV \to \sigma^h \frac{\partial \epsilon^h}{\partial T_s} dS , \quad \text{(A3)}$$

$$\gamma^e \varphi^e dV \to \Gamma^e \varphi^e dS, \quad \gamma^h \varphi^h dV \to \Gamma^h \varphi^h dS , \quad \text{(A4)}$$

$$\rho^e \vec{E}^e_{rd} \cdot \vec{v}^e dV \to \rho^e f^e_{rd} \vec{n} \cdot \vec{v}^e dS ,$$

$$\rho^h \vec{E}^h_{rd} \cdot \vec{v}^h dV \to \rho^h f^h_{rd} \vec{n} \cdot \vec{v}^h dS , \quad \text{(A5)}$$

$$\rho^e E^e_{dn} v^e_n dV \to \rho^e f^e_d v^e_n dS ,$$

$$\rho^h E^h_{dn} v^h_n dV \to \rho^h f^h_d v^h_n dS , \quad \text{(A6)}$$

$$\rho^e E^e_{dt} v^e_t dV \to \sigma^e E^e_{dt} v^e_t dS ,$$

$$\rho^h E^h_{dt} v^h_t dV \to \sigma^h E^h_{dt} v^h_t dS , \quad \text{(A7)}$$

$$g \, dV \to g_s dS , \quad \text{(A8)}$$

where ϵ^s is the stored internal energy per unit area of the macroscopic lattice interface, σ^e, σ^h, Γ^e, and Γ^h are the surface-charge densities and surface-charge source densities for the conduction electron and hole fluids, respectively, the surface forces per unit charge density per unit area f^e and f^h are split into purely dissipative and inseparably mixed recoverable-dissipative contributions (discussed below), and T_s is the surface temperature, which is assumed equal to the uniform bulk temperature T in this paper. The n and t subscripts indicate vector components normal and tangential to the surface whose differential element of area is given by dS. The surface-energy source density g_s in (A8) accounts for radiant energy, e.g., involved in surface photoexcitation of carriers, and we have assumed that the volumetric polarization $\vec{P}$ remains bounded.

Now, employing the surface-charge balance equations[47] [deduced from the integral forms (3.1), (3.2), and (3.3) of Ref. 1]

$$\begin{aligned}&\frac{\partial\sigma^e}{\partial t}+\vec{n}\cdot[\rho^e\vec{v}^{\,e}]=\Gamma^e\,,\\&\frac{\partial\sigma^h}{\partial t}+\vec{n}\cdot[\rho^h\vec{v}^{\,h}]=\Gamma^h\,,\\&\frac{\partial\sigma^i}{\partial t}=\Gamma^i\,,\end{aligned}\tag{A9}$$

the fact that the carrier velocities, charge densities, and charge-generation terms are negligible or vanish in the insulator, (A2)–(A8), and the arbitrariness of the portion of the interface enclosed by V, we obtain

$$\frac{d\epsilon^s}{dt}+\left[\sigma^e\frac{\partial\epsilon^e}{\partial T_s}+\sigma^h\frac{\partial\epsilon^h}{\partial T_s}\right]\frac{dT_s}{dt}+f^e_{\rm rd}\frac{d\sigma^e}{dt}+f^h_{\rm rd}\frac{d\sigma^h}{dt}$$
$$=-\rho^e f^e_{\rm d}v^e_{\rm n}-\rho^h f^h_{\rm d}v^h_{\rm n}-\sigma^e E^e_{\rm t}v^e_{\rm t}-\sigma^h E^h_{\rm t}v^h_{\rm t}-\Gamma^e(\varphi^e-f^e_{\rm rd})-\Gamma^h(\varphi^h-f^h_{\rm rd})+g_s\,,\tag{A10}$$

where the d subscripts on $\vec{E}^{\,e}$ and $\vec{E}^{\,h}$ [from (A7)] have been omitted since these quantities are purely dissipative. Equation (A10) is a particularly convenient form of the first law of thermodynamics for the semiconductor-insulator interface.

The second law of thermodynamics for the surface, i.e., the existence of a surface-entropy function and the fact that the rate of surface-entropy production is greater than or equal to zero, cannot be implemented in the same way as was done in the volumetric case treated in Ref. 1 because of the fact that the mixed surface-force terms $f^e_{\rm rd}$ and $f^h_{\rm rd}$ cannot be separated into sums of recoverable and dissipative parts. Instead, following the existing procedures for generalizing[48] the definition of entropy to a path-dependent function, we postulate the existence of a surface-entropy density η_s and define the non-negative rate of production of entropy per unit area by

$$\gamma_s=\frac{d\eta_s}{dt}-\frac{g_s}{T_s}\,,\tag{A11}$$

where, again, $T_s=T$ for this work. Now, substituting from (A10) into (A11), we find

$$\gamma_s=\frac{d\eta_s}{dt}-\frac{1}{T_s}\frac{d\epsilon^s}{dt}+\frac{1}{T_s}\left[\left[\sigma^e\frac{\partial\epsilon^e}{\partial T_s}+\sigma^h\frac{\partial\epsilon^h}{\partial T_s}\right]\frac{dT_s}{dt}+f^e_{\rm rd}\frac{d\sigma^e}{dt}+f^h_{\rm rd}\frac{d\sigma^h}{dt}+\rho^e f^e_{\rm d}v^e_{\rm n}+\rho^h f^h_{\rm d}v^h_{\rm n}\right.$$
$$\left.+\sigma^e\vec{E}^{\,e}_{\rm t}\cdot\vec{v}^{\,e}_{\rm t}+\sigma^h\vec{E}^{\,h}_{\rm t}\cdot\vec{v}^{\,h}_{\rm t}+\Gamma^e(\varphi^e-f^e_{\rm rd})+\Gamma^h(\varphi^h-f^h_{\rm rd})\right]\geq 0\,,\tag{A12}$$

which is the rate of surface-entropy production inequality (or Clausius-Duhem inequality) for the semiconductor-insulator interface.[48]

At this point it may be helpful and of interest to comment on the meaning of some of the terms in (A10) and (A12), first considering those descriptive of the energy dissipation and entropy production due to the flow of charge carriers at the surface. Flows parallel to the interface, i.e., the surface currents $\sigma^e\vec{v}^{\,e}_{\rm t}$ and $\sigma^h\vec{v}^{\,h}_{\rm t}$, dissipate energy through the terms $\sigma^e\vec{E}^{\,e}_{\rm t}\cdot\vec{v}^{\,e}_{\rm t}$ and $\sigma^h\vec{E}^{\,h}_{\rm t}\cdot\vec{v}^{\,h}_{\rm t}$. These account for Ohmic-type losses quite similar to those produced by volumetric currents. The normal current densities $\rho^e v^e_{\rm n}$ and $\rho^h v^h_{\rm n}$ instead dissipate according to the $\rho^e f^e_{\rm d}v^e_{\rm n}$ and $\rho^h f^h_{\rm d}v^h_{\rm n}$ terms, which account for energy dissipation produced as the charged fluids are decelerated from their nonzero macroscopic velocities in the interior ($x=0^+$) to zero velocity at the

interface ($x=0$). Next, we consider the dissipation produced through the surface-charge source densities Γ^e and Γ^h. In the interior of the semiconductor the conduction-electron charge source density dissipates energy according to $-\gamma^e\varphi^e$, i.e., the amount of electron charge destroyed per unit volume per unit time, $-\gamma^e$, times the energy per unit charge, φ^e, equals the energy dissipated. At the surface the prescription is not as straightforward because the interface is capable of storing recoverable energy. Consequently, the total energy dissipated per unit charge at the interface through the electron surface-charge source density is equal to the difference between the incoming energy per unit charge φ^e and the energy per unit charge stored by the interface $f^e_{\rm rd}$ (we are discussing $f^e_{\rm rd}$ here under the circumstance that it is purely recoverable) multiplied by the electron surface-charge source density Γ^e. A similar explanation holds for the term $\Gamma^h(\varphi^h-f^h_{\rm rd})$.

Now, the surface constitutive theory cannot be developed in the same way as it was volumetrically because we do not have a state-function equation for the surface analogous to (A6) of Ref. 1. Again, this is a consequence of the inability to separate $f^e_{\rm rd}$ and $f^h_{\rm rd}$ into recoverable and dissipative parts. Instead, we first assert that no possible field dependences may be excluded *a priori*,[49] and from (A12) we write

$$\begin{aligned}
&\epsilon_{\rm sem}=\epsilon_{\rm sem}(\sigma^e,\sigma^h,\rho^e,\rho^h,\vec{\rm v}^{\,e},\vec{\rm v}^{\,h},\vec{\rm E},T)\ ,\\
&\Gamma^e=\Gamma^e(\sigma^e,\sigma^h,\rho^e,\rho^h,\vec{\rm v}^{\,e},\vec{\rm v}^{\,h},\vec{\rm E},T)\ ,\\
&\Gamma^h=\Gamma^h(\sigma^e,\sigma^h,\rho^e,\rho^h,\vec{\rm v}^{\,e},\vec{\rm v}^{\,h},\vec{\rm E},T)\ ,
\end{aligned}\tag{A13}$$

$$\begin{aligned}
&f^e_{\rm rd}=f^e(\sigma^e,\sigma^h,\rho^e,\rho^h,\vec{\rm v}^{\,e},\vec{\rm v}^{\,h},\vec{\rm E},T)\ ,\\
&f^e_{\rm d}=f^e_{\rm d}(\sigma^e,\sigma^h,\rho^e,\rho^h,\vec{\rm v}^{\,e},\vec{\rm v}^{\,h},\vec{\rm E},T)\ ,\\
&f^h_{\rm rd}=f^h(\sigma^e,\sigma^h,\rho^e,\rho^h,\vec{\rm v}^{\,e},\vec{\rm v}^{\,h},\vec{\rm E},T)\ ,\\
&f^h_{\rm d}=f^h_{\rm d}(\sigma^e,\sigma^h,\rho^e,\rho^h,\vec{\rm v}^{\,e},\vec{\rm v}^{\,h},\vec{\rm E},T)\ ,
\end{aligned}\tag{A14}$$

where ρ^e, ρ^h, $\vec{\rm v}^{\,e}$, $\vec{\rm v}^{\,h}$, and T are, of course, evaluated at the interface and $\vec{\rm E}$ indicates possible dependences on the Maxwell electric field on either side of the interface. Now, the form of (A12) indicates that $f^e_{\rm rd}$ and $f^h_{\rm rd}$ are primarily dependent on σ^e and σ^h, respectively. However, because constitutive equations containing these surface variables would be difficult to implement and because σ^e and σ^h are presumed to depend primarily on ρ^e and ρ^h, respectively, we omit an explicit dependence on σ^e and σ^h from all equations in (A13) and (A14). Also, we will assume that the forces exerted by the macroscopic lattice surface on the electron (hole) fluid are, to a good approximation, independent of hole (electron) variables, thus excluding the dependence of $f^e_{\rm rd}$ and $f^e_{\rm d}$ on ρ^h and $\vec{\rm v}^{\,h}$ and of $f^h_{\rm rd}$ and $f^h_{\rm d}$ on ρ^e and $\vec{\rm v}^{\,e}$. Hence, we rewrite (A14) as

$$\begin{aligned}
&f^e_{\rm rd}=f^e_{\rm rd}(\rho^e,\vec{\rm v}^{\,e},\vec{\rm E},T),\\
&f^h_{\rm rd}=f^h_{\rm rd}(\rho^h,\vec{\rm v}^{\,h}\vec{\rm v}^{\,h},\vec{\rm E},T)\ ,\\
&f^e_{\rm d}=f^e_{\rm d}(\rho^e,\vec{\rm v}^{\,e},\vec{\rm E},T),\\
&f^h_{\rm d}=f^h_{\rm d}(\rho^h,\vec{\rm v}^{\,h}\vec{\rm E},T)\ .
\end{aligned}\tag{A15}$$

The constitutive forms in (A13) and (A15) are, in general, arbitrary functionals over the histories of the variables shown, which are restricted, as in the bulk, by constraints set by the inequality (A12). Further specification of these functions is based simply on agreement with experiment. In this paper we have found it convenient to divide f^e and f^h into three parts each: purely recoverable, purely dissipative, and mixed recoverable-dissipative. The first and last of these, together, constitute $f^e_{\rm rd}\equiv f^e_0+f^e_m$ and $f^h_{\rm rd}\equiv f^h_0+f^h_m$. The portions of f^e and f^h that do not vanish in static cases are, of course, purely recoverable and are designated f^e_0 and f^h_0. Clearly, the functional forms are

$$f^e_0=f^e_0(\rho^e,\vec{\rm E},T),\quad f^h_0=f^h_0(\rho^e,\vec{\rm E},T)\ .\tag{A16}$$

Particular forms for these functions were discussed in Ref. 1. The remaining portions of f^e and f^h are termed f^e_1 and f^h_1 and for purposes of convenience are further split. The parts not vanishing in dc cases (but zero, in static situations) must be purely dissipative and are labeled $f^e_{\rm d}$ and $f^h_{\rm d}$. As seen above, they act much like the (purely dissipative) bulk quantities $\vec{\rm E}^{\,e}$ and $\vec{\rm E}^{\,h}$ and, as in the bulk, the simplest choice for $f^e_{\rm d}$ and $f^h_{\rm d}$ is linearly proportional to the respective velocities, i.e.,

$$f^e_{\rm d}=\vec{\rm A}^{\,D}\cdot\vec{\rm v}^{\,e},\quad f^h_{\rm d}=\vec{\rm D}^{\,D}\cdot\vec{\rm v}^{\,h}\ .\tag{A17}$$

It is noted that (A12) requires that $\vec{\rm A}^{\,D}<0$ and $\vec{\rm D}^{\,D}>0$ (in the same way that considerations of volumetric entropy production constrain bulk mobilities to be positive). Lastly, the parts of f^e and f^h present only in ac and transient situations, designated f^e_m and f^h_m, are inseparable mixtures of recoverable and dissipative components. The form of (A12) suggests that f^e_m and f^h_m be selected as linear functionals (integrals) over the histories of the time rates of change of the electron and hole charge densities, respectively, and such a choice appears sufficient to account for experimental observation.

APPENDIX B: ADMITTANCE ANALYSIS FOR DEPLETION AND INVERSION

As indicated in Sec. IV, in order to include the influence on the admittance of the $d\varphi_1/dx\,|_{\rm sem}$ (the small electric field at $x=0$) and $E(\omega)$ and $H(\omega)$

terms appearing in the semiconduction boundary conditions, (4.22) and (4.23), and to incorporate the effects of carrier generation in the depletion layer in the analysis of the inversion situation, it is essential to solve the problem posed in Sec. IV in the space-charge layer as well as in the charge-neutral region. In order to do this and still obtain analytical expressions for the admittance, we approximate the non-constant coefficients ρ_0^e, ρ_0^h, and E_0 appearing in the differential equations (4.4) and (4.5) by step functions. An approximate solution to the original system is then obtained by solving the equations in each region and matching the solutions by satisfying certain continuity conditions across each step discontinuity. Obviously, by including many such steps arbitrary accuracy is obtainable. However, in this paper where the focus is on qualitative and rough quantitative discussion, two or three steps are deemed to be sufficient.[50] The nature of the approximation technique requires separate analyses of the depletion and inversion situations, which we perform here for n-type material.

Now, in the treatment of depletion we split the epilayer into three sections with the static solution being approximated as follows: In the bulk

$$\rho_0^e \equiv \rho_b^e \gg \rho_0^h \equiv \rho_b^h , \quad \frac{d\varphi_0}{dx}=0, \quad L \le x \le h \tag{B1}$$

while in the depletion layer,

$$\rho_0^e \equiv \rho_d^e \gg \rho_0^h \equiv \rho_d^h , \quad \frac{d\varphi_0}{dx}=\frac{-\varphi_s}{L}, \quad 0 < x \le L \tag{B2}$$

and at the surface

$$\rho_0^e \equiv \rho_s^e \gg \rho_0^h \equiv \rho_s^h, \quad x=0 \tag{B3}$$

where L is roughly the Debye length, φ_s is the surface potential, and we permit ρ_s^e and ρ_s^h to differ from ρ_d^e and ρ_d^h for greater flexibility in representing the actual $\rho_0^e(x)$ and $\rho_0^h(x)$. In order to maintain a faithful rendering of the influence of the vital semiconduction boundary conditions that contain ρ_0^e at $x=0$ and ρ_0^h at $x=0$, we take ρ_s^e and ρ_s^h to be the actual static surface values satisfying

$$\rho_s^e=\rho_b^e \exp\left[\frac{\mu\varphi_s}{D}\right], \quad \rho_s^h=\rho_b^h \exp\left[\frac{-\mu\varphi_s}{D}\right] . \tag{B4}$$

The displacement current in the bulk may be neglected at all frequencies of interest; consequently, $J^e+J^h \cong 1$ for $L<x<h$. Then, from (4.4)–(4.9) with (B1), the charge-neutrality assumption [Eq. (3.13)], and (2.11) with $G \equiv 0$, the solution in the bulk is readily found to be

$$\rho_1^h=-\rho_1^e=C_0(e^{x/L_p}-e^{(2h-x)/L_p}) , \tag{B5a}$$

$$J^h=1-J^e=\frac{-D^h}{L_p}C_0(e^{x/L_p}+e^{(2h-x)/L_p}) , \tag{B5b}$$

$$\varphi_1=\frac{1}{\mu^e\rho_b^e}[x-h+(D^h-D^e)\rho_1^h] , \tag{B5c}$$

where $L_p \equiv (D^h\tau_p)^{1/2}$ is the diffusion length for holes and the condition on ρ_1^h at $x=h$ [Eq. (4.12)] has been utilized. Next, in the depletion layer (4.4) and (4.5) with (4.2), (4.6), and (4.7) with $\gamma^h=0$ (since $L_p \gg L$) and (4.8) are easily solved (with displacement current across the depletion layer included to first order by iteration) and yield

$$\rho_1^h=\frac{LC_1}{\mu^h\varphi_s}+C_2e^{\bar{\varphi}_s x/L} , \tag{B6a}$$

$$\rho_1^e=-\frac{LC_1}{\mu^h\varphi_s}-\frac{L^2\mu\rho_d^eC_2e^{\bar{\varphi}_s x/L}}{D\epsilon_{\rm sem}N}+C_3e^{m_1x/L}+C_4e^{m_2x/L} , \tag{B6b}$$

$$J^h=C_1, \quad J^e=1-C_1+\frac{i\omega\epsilon_{\rm sem}\varphi_sC_4}{L\rho_d^e} , \tag{B6c}$$

$$\varphi_1=C_5+\left[\frac{1-C_1}{D^e}-\frac{C_1}{D^h}\right]\frac{Dx}{\mu\rho_d^e}+\frac{D}{\mu\rho_d^e}\left[\frac{\bar{\varphi}_s+m_1}{m_1}C_3e^{m_1x/L}+\frac{\bar{\varphi}_s+m_2}{m_2}C_4e^{m_2x/L}\right]-\frac{2L^2C_2e^{\bar{\varphi}_s x/L}}{\epsilon_{\rm sem}N} , \tag{B6d}$$

where

$$\bar{\varphi}_s=\frac{\mu}{D}\varphi_s, \quad N=2\bar{\varphi}_s^2+\frac{\mu\rho_d^eL^2}{D\epsilon_{\rm sem}}$$

and

$$m_1,m_2=\frac{-\bar{\varphi}_s}{2}\pm\frac{1}{2}\left[\bar{\varphi}_s^2-\frac{4\mu\rho_d^e L^2}{D\epsilon_{\rm sem}}\right]^{1/2}.$$

The solutions in the two regions are matched by requiring the continuity of J^h, ρ_1^e, ρ_1^h, and φ_1 at $x=L$. The four resulting conditions plus the two semiconduction boundary conditions (4.14) and (4.15) then enable the determination of the six integration constants $C_0,\ldots,C_5$. The continuity conditions for J^h, ρ_1^e, ρ_1^h, and φ_1 yield

$$\frac{-D^h}{L_p}C_0(1+e^{2h/L_p})=C_1\ , \tag{B7a}$$

$$-C_0(1-e^{2h/L_p})=C_3e^{m_1}+C_4e^{m_2}\ , \tag{B7b}$$

$$C_0(1-e^{2h/L_p})=C_2e^{\bar{\varphi}_s}\ , \tag{B7c}$$

$$\frac{-h}{\mu^e\rho_b^e}+\frac{D^h-D^e}{\mu^e\rho_b^e}C_0(1-e^{2h/L_p})=C_5+\frac{D}{\mu\rho_d^e}\left[\frac{\bar{\varphi}_s+m_1}{m_1}C_3e^{m_1}+\frac{\bar{\varphi}_s+m_2}{m_2}C_4e^{m_2}\right], \tag{B7d}$$

where the facts that L_p and h are much larger than L have been employed. The two semiconduction boundary conditions (4.14) and (4.15) along with (B6) yield

$$\frac{A_1 i}{\omega\epsilon_{\rm ox}}+\frac{DA_2}{L\mu\rho_d^e}[(\bar{\varphi}_s+m_1)C_3+(\bar{\varphi}_s+m_2)C_4]+\frac{A_e}{\rho_s^e}(C_3+C_4)-\frac{1-C_1}{\nu^e\rho_s^e}-\frac{i\omega\epsilon_{\rm sem}\varphi_s C_4}{L\rho_d^e\nu^e\rho_s^e}=0\ , \tag{B8}$$

$$\frac{A_1 i}{\omega\epsilon_{\rm ox}}+\frac{DA_2}{L\mu\rho_d^e}[(\bar{\varphi}_s+m_1)C_3+(\bar{\varphi}_s+m_2)C_4]-\frac{A_h}{\rho_s^h}C_2+\frac{C_1}{\nu^h\rho_s^h}=0\ . \tag{B9}$$

The influence of ρ_1^h on φ_1 and ρ_1^e in the space-charge region has been neglected in (B7)–(B9), since this is clearly a secondary effect. This amounts to neglecting the first two terms in (B6b) and the last term of (B6d). We may also omit the left-hand side of (B7d) [as well as the second term in (B6d)], which carries the contributions to φ_1 produced by the bulk resistance to electron flow and by relative diffusion effects, i.e., the diffusion voltage. In addition, for depletion with $\bar{\varphi}_s\lesssim -3$ we may assume that $\bar{\varphi}_s^2 >> -4\mu\rho_d^e L^2/D\epsilon_{\rm sem}$, i.e., the static field moving dynamic charge dominates over the dynamic field pushing static charge, so that $m_1\approx-\bar{\varphi}_s$, $m_2\approx-\mu\rho_d^e L^2/D\epsilon_{\rm sem}\bar{\varphi}_s$, and $\bar{\varphi}_s+m_1\cong -m_2$. Since $|m_1| >> |m_2|$, it is also reasonable to assume that $(\bar{\varphi}_s+m_1)C_3$ is negligible compared with $(\bar{\varphi}_s+m_2)C_4$, hence simplifying (B7d), (B8), and (B9). This may be verified *a posteriori*. Incorporating all of the above into the solution of (B7)–(B9) we can show, using (B6d) that

$$\varphi_1(x=0)\simeq\left[\frac{A_2\epsilon_{\rm ox}}{A_1L}+\frac{A_e\rho_d^e\nu^e}{\omega_D\varphi_s}+\frac{i\omega\epsilon_{\rm sem}}{\omega_D L}\right]^{-1}\times\left[\frac{i-\omega/\omega_D}{\omega}\right], \tag{B10}$$

where

$$\omega_D=\frac{A_1\nu^e\rho_s^e}{\epsilon_{\rm ox}}+\frac{A_1\rho_b^h}{\epsilon_{\rm ox}A_h}\left[\frac{-\rho_b^h}{A_h\nu^h\rho_s^h}+\frac{L_p}{D^h}\tanh\frac{h}{L_p}\right]^{-1},$$

and the admittance Y is then obtained with the aid of (4.25) and takes the form

$$Y(\omega_0)\simeq -a\omega_0\left[\frac{A_2\epsilon_{\rm ox}}{A_1L}+\frac{A_e\rho_d^e\nu^e}{\omega_D\varphi_s}+\frac{i\omega\epsilon_{\rm sem}}{\omega_D L}\right]\times\left[\frac{i+\omega_0/\omega_D}{1+\omega_0^2/\omega_D^2}\right]. \tag{B11}$$

Since ρ_d^e and L are not precisely defined, the amplitude of Y_p given in (B11) is not precise. However, the accuracy may be "maximized" through an "optimum" selection of values for ρ_d^e and L. A way of doing this is to note that when $\omega_0\to 0$ and $\nu^e,\nu^h,\tau_p\to\infty$ the result must reduce (when divided by $i\omega_0$) to the static differential capacitance of the MOS structure with the oxide contribution subtracted off, which may be written

$$C=-\frac{d\sigma_s}{d\varphi_s}-\epsilon_{\rm sem}d\left[\left.\frac{d\varphi_0}{dx}\right|_{\rm sem}\right]\Big/d\varphi_s\ ,$$

where σ_s, the surface-charge density at the Si-SiO_2

interface is given in (2.14). Since in the static limit $A_e \to A^s$ and from (B2)

$$d\left[\left.\frac{d\varphi_0}{dx}\right|_{\text{sem}}\right]\Big/ d\varphi_s = -1/L \ ,$$

one can show that ρ_d^e should equal $-\rho_s^e \bar{\varphi}_s$, with which[51]

$$Y = a\omega_0 \left[\frac{A_2 \epsilon_{\text{ox}}}{A_1} \frac{d}{d\varphi_s} \left[\left. \frac{d\varphi_0}{dx} \right|_{\text{sem}} \right] - \frac{A_e \rho_s^e \nu^e \mu}{\omega_D D} + \frac{i\omega \epsilon_{\text{sem}}}{\omega_D L} \right] \times \left[\frac{i + \omega_0/\omega_D}{1 + \omega_0^2/\omega_D^2} \right] . \tag{B12}$$

Equation (B12) is introduced and discussed in Sec. IV.

In a similar treatment of the case of inversion the existence of the inversion layer necessitates the introduction of an additional constant coefficient region. The static charge densities and electric field for the bulk are again given by (B1), while the space-charge region of width L, made up of depletion and inversion layers, is approximated as follows: In the depletion region (of width $L_d \equiv L - L_s$),

$$\begin{aligned} &\rho_0^e \equiv \rho_d^e \sim \rho_0^h \equiv \rho_d^h \ , \\ &\frac{d\varphi_0}{dx} = \frac{-\varphi_0}{L_d}, \quad L_s \le x \le L \end{aligned} \tag{B13}$$

while for the inversion layer (of width L_s)

$$\begin{aligned} &\rho_0^e \equiv \rho_i^e \ll \rho_0^h \equiv \rho_i^h \ , \\ &\frac{d\varphi_0}{dx} = \frac{-\varphi_i}{L_s}, \quad 0 < x \le L_s \ . \end{aligned} \tag{B14}$$

The drops in φ_0 across the two layers are given by φ_d and φ_i, respectively, with, at least for weak inversion, $\varphi_d + \varphi_i = \varphi_s$ ($\equiv$surface potential). At the surface we again assume (B3) with (B4) where ρ_s^e and ρ_s^h need not equal ρ_i^e and ρ_i^h. Finally, we may neglect the displacement current everywhere except in the high-resistivity depletion layer.

The solution in the bulk region is identical with that in the case of depletion, i.e., (B5). Next, treating the depletion-layer problem, we assume that because of the relatively high resistivity of the region, we can neglect the terms $\mu^e \rho_d^e d\varphi_1/dx$ and $\mu^h \rho_d^h d\varphi_1/dx$ appearing in (4.4) and (4.5), respectively, and the right-hand side of (4.8), thus uncoupling the problem for φ_1.[52] Integration of (4.8) then yields

$$\varphi_1 = C_2 x + C_3, \quad L_s \le x \le L \ . \tag{B15}$$

To solve for ρ_1^e, ρ_1^h, J^e, and J^h, we assume that the charge-source densities in (4.6) and (4.7) are given by the linear form

$$\gamma^h = \frac{\rho_1^e - \rho_1^h}{\tau}, \quad L_s \le x \le L \ . \tag{B16}$$

Assuming that $L_d^2 e^{-\bar{\varphi}_d}/\bar{\varphi}_d^2 D^e \tau \ll 1$, which essentially means that the electric field in the depletion layer is large enough to sweep most of the generated carriers from the layer, we may obtain an approximate solution to (4.4)–(4.7) with (B13) and (B16) by iteration, and find

$$\rho_1^e = \frac{-C_1 L_d}{D^e \bar{\varphi}_d} + C_4 e^{-\bar{\varphi}_d x/L_d} \ , \tag{B17a}$$

$$\rho_1^h = \frac{C_{11} L_d}{\bar{\varphi}_d D^h} + C_5 e^{\bar{\varphi}_d x/L_d}, \quad L_s \le x \le L \tag{B17b}$$

$$J^e = C_1 + \frac{L_d}{\bar{\varphi}_d \tau} \left[\left(\frac{C_{11}}{D^h} + \frac{C_1}{D^e} \right) x + C_4 e^{-\bar{\varphi}_d x/L_d} + C_5 e^{\bar{\varphi}_d x/L_d} \right] , \tag{B17c}$$

$$J^h = C_{11} - \frac{L_d}{\bar{\varphi}_d \tau} \left[\left(\frac{C_{11}}{D^h} + \frac{C_1}{D^e} \right) x + C_4 e^{-\bar{\varphi}_d x/L_d} + C_5 e^{\bar{\varphi}_d x/L_d} \right] . \tag{B17d}$$

Finally, in the inversion layer the problem is identical with the surface-layer problem of the depletion case with holes rather than electrons now being the dominant carrier. Paralleling the earlier treatment, we may neglect the charge-source density γ^h, since $L_s \ll (D^e \tau_n)^{1/2}$, and ignore the influence of ρ_1^e on φ_1 and ρ_1^h, i.e., neglect ρ_1^e in the charge equation (4.8). Then, solving (4.4)–(4.8) with (B14), we obtain

$$\rho_1^e = \frac{-L_s(1 - C_{10})}{D^e \bar{\varphi}_i} + C_6 e^{-\bar{\varphi}_i x/L_s} \ , \tag{B18a}$$

$$\rho_1^h = C_7 e^{n_1 x/L_s} + C_8 e^{n_2 x/L_s}, \quad 0 \le x \le L_s \tag{B18b}$$

$$J^h = 1 - J^e = C_{10} \ , \tag{B18c}$$

$$\varphi_1 = C_9 + \left(\frac{1 - C_1}{D^e} + \frac{C_1}{D^h} \right) \frac{Dx}{\mu \rho_i^h} + \frac{D}{\mu \rho_i^h} \left[\frac{\bar{\varphi}_i - n_1}{n_1} C_7 e^{n_1 x/L_s} + \frac{\bar{\varphi}_i - n_2}{n_2} C_8 e^{n_2 x/L_s} \right] , \tag{B18d}$$

where

$$n_1,n_2=\frac{\bar{\varphi}_i}{2}\pm\frac{1}{2}\left[\bar{\varphi}_i^2+\frac{4\mu\rho_i^h L_s^2}{D\epsilon_{\rm sem}}\right]^{1/2}.$$

The continuity conditions employed in order to connect the solution functions in the three regions together are the continuity of ρ_1^e, ρ_1^h, J^h, J_T (the total current), and φ_1 at $x=L$ and ρ_1^e, ρ_1^h, J^h, φ_1, and $d\varphi_1/dx$ at $x=L_s$. These ten plus the two semiconduction boundary conditions determine the twelve integration constants $C_0,\ldots,C_{11}$. In solving this system, as before, we neglect the contributions to φ_1 (in all regions) arising from relative diffusion effects and from resistance to dominant carrier flow. In addition, we exploit the facts that $h,L_p\gg L_s,L_d$ and that for inversion $\bar{\varphi}_i^2\gg 4\mu\rho_i^h L_s^2/D\epsilon_{\rm sem}$, from which it follows that

$$n_1\simeq\bar{\varphi}_i,\quad n_2\simeq\frac{-\mu\rho_i^h L_s^2}{D\epsilon_{\rm sem}\bar{\varphi}_i},\qquad \bar{\varphi}_i-n_1\simeq n_2\ . \tag{B19}$$

Using an argument similar to that employed in the depletion case, since $|n_2|\ll|n_1|$, it is reasonable to assume that n_2C_7 is negligible compared to $\bar{\varphi}_iC_8$. The semiconduction boundary conditions (4.22) and (4.23) now take the respective forms

$$\frac{A_1 i}{\omega\epsilon_{\rm ox}}+\frac{\varphi_i C_8}{\rho_i^h L_s}A_2+\frac{A_e}{\rho_s^e}\left[C_6-\frac{L_s(1-C_{10})}{\mu^e\varphi_i}\right]-\frac{1-C_{10}}{\nu^e\rho_s^e}=0\ , \tag{B20}$$

$$\frac{A_1 i}{\omega\epsilon_{\rm ox}}+\frac{\varphi_i C_8}{\rho_i^h L_s}A_2-\frac{A_h}{\rho_s^h}(C_7+C_8)=0\ , \tag{B21}$$

where in reaching (B21) we have neglected the current term from (4.23) since ρ_s^h is large. This assumption—note that the remaining terms in (B21) are recoverable [$H(\omega)$ is negligible for inversion]—is equivalent to the physical assertion that when ρ_s^h is large the interface exerts force quasistatically on the hole gas.

Employing all of the above-mentioned approximations, we find the eleven constants $C_0,\ldots,C_{10}$ from which, omitting the algebra, φ_1 at $x=0$ is obtained from (B18d),

$$\varphi_{1s}\simeq\frac{i-\omega_0/\omega_I}{\omega_0}\left[\frac{A_2\epsilon_{\rm ox}}{A_1 L}+\frac{\epsilon_{\rm ox}A_h\rho_i^h L_s e^{-\bar{\varphi}_i}}{A_1 L\varphi_i\rho_s^h}\times\frac{\rho_b^h/A_h\nu^e\rho_s^e}{(\rho_b^h/A_h)(1/\nu^e\rho_s^e)+[(D^h/L_p)\coth(h/L_p)-(L_d/\bar{\varphi}_d\tau)e^{-\bar{\varphi}_d}]^{-1}}+\frac{i\omega_0\epsilon_{\rm sem}}{\omega_I L_d}\right]^{-1}, \tag{B22}$$

where

$$\omega_I\simeq\frac{A_1\rho_b^h}{\epsilon_{\rm ox}A_h}\left[\frac{A_h\nu^e\rho_s^e}{\rho_b^h}+\frac{D^h}{L_p}\coth\frac{h}{L_p}-\frac{L}{\bar{\varphi}_d\tau}e^{-\bar{\varphi}_d}\right].$$

Exactly as in the depletion case, since L, L_s, φ_i, and ρ_i^h are not precisely known, the expression for φ_{1s} [Eq. (B22)] is only approximate. Again we can optimize the approximation by examining the static limit of (B22), i.e., by letting $\omega_0,\tau,\nu^h,\tau_p\to 0$. Since $A_h\to A^s$ we should have

$$d\left[\left.\frac{d\varphi_0}{dx}\right|_{\rm sem}\right]\Big/d\varphi_s=-\frac{1}{L}$$

and $\rho_i^h=L\varphi_i\rho_s^h\exp(\bar{\varphi}_i)/L_s$, with which we may write

$$Y=\frac{a\omega_0(i+\omega_0/\omega_I)}{1+\omega_0^2/\omega_I^2}\left[-\frac{A_2\epsilon_{\rm ox}}{A_1}\frac{d}{d\varphi_s}\left[\left.\frac{d\varphi_0}{dx}\right|_{\rm sem}\right]+\frac{\mu\epsilon_{\rm ox}A_h}{DA_1}\left[\frac{\rho_b^h/A_h\nu^e\rho_s^e}{(\rho_b^h/A_h)(1/\nu_e\rho_s^e)+[(D^h/L_p)\coth(h/L_p)-(L_d/\bar{\varphi}_d\tau)e^{-\bar{\varphi}_d}]^{-1}}\right]+\frac{i\omega_0\epsilon_{\rm sem}}{\omega_I L_d}\right]. \tag{B23}$$

This expression is discussed in Sec. IV.

*Present address: Naval Research Laboratory, Code 6813, Washington, D.C. 20375.

[1]M. G. Ancona and H. F. Tiersten, Phys. Rev. B 22, 6104 (1980).

[2]In Appendix A of this paper (see Ref. 1 also) it is argued that the surface force functions should be functions of the electric field on each side of the interface and of the respective charge densities and velocities of each fluid at the surface as well as possible dependences on the time derivatives of any of these quantities.

[3]See, for example, W. Shockley, *Electrons and Holes in Semiconductors* (Van Nostrand, Princeton, N.J., 1950).

[4]A. H. Nayfeh, *Perturbation Methods* (Wiley, New York, 1973).

[5]W. Shockley, Bell Syst. Tech. J. 28, 435 (1949).

[6]Quasimicroscopic justifications have been given, e.g., by J. P. McKelvey, *Solid State and Semiconductor Physics* (Harper and Row, New York, 1966), p. 346. However, these studies argue the plausibility of such a condition and not on its consistency with the rest of the field description.

[7]This has previously been recognized in the context of the quasimicroscopic Shockley-Read-Hall model of an interface; see, e.g., A. Many, Y. Goldstein, and N. B. Grover, *Semiconductor Surfaces* (Wiley, New York, 1965), p. 197. It is noted, however, that their low-level expressions differ considerably from those we derive. Also, the existence of and need to relate to *two* boundary conditions for large-signal cases is completely ignored by their treatment. See also Ref. 37.

[8]The Shockley approach has often been applied to transient problems for the determination of surface-recombination velocities. As has been noted by A. Many, Y. Margoninski, E. Harnik, and E. Alexander [Phys. Rev. 101, 1433 (1956)] and as argued in Sec. III and in Ref. 33, only when applied after the initial "rapid" decay is such an analysis sensible. To discuss the full transient the problem in the space-charge region must be addressed—see Sec. III for further details.

[9]See, for example, D. VanDorpe, J. Borel, G. Merckel, and P. Saintot, Solid State Electron. 15, 547 (1972).

[10]K. Lehovec and A. Slobodskoy, Solid State Electron. 7, 59 (1964).

[11]E. H. Nicollian and A. Goetzberger, Bell Syst. Tech. J. 46, 1055 (1967).

[12]D. H. Eaton and C. T. Sah, Phys. Status Solidi 12, 95 (1972).

[13]The surface-force functions are actually functions of temperature. Since in this paper only isothermal cases are treated, we omit explicit indications of this in all equations [except Eqs. (2.17) and (2.18) and in Appendix A].

[14]See Appendix B of Ref. 1. The quantities in (2.17) and (2.18) are actually $\hat{\varphi}^e$ and $\hat{\varphi}^h$ of Ref. 1. The quantities N_c and N_v are the quasimicroscopic "effective densities of states" for the conduction and valence bands, respectively.

[15]See Appendix A of this paper and of Ref. 1 for some discussion of the meaning of these coefficients.

[16]This change plus an inconsequential change in the form of the logarithmic terms in (2.19) and (2.20) make the numerical values of the A_i coefficients of Ref. 1 and those of this paper different but, of course, trivially related.

[17]S. M. Sze, *Physics of Semiconductors* (Wiley, New York, 1969), p. 468, and Appendix B of Ref. 1.

[18]C. A. Hogarth, in *Progress in Semiconductors,* edited by A. F. Gibson (Wiley, New York, 1956), Vol. I.

[19]See, for example, J. P. McKelvey, (cited in Ref. 6), p. 351. Note that in our work the assumption associated with (2.35) is required for the decoupling.

[20]This view is adopted because in this paper we wish to examine only surface effects acting normal to the interface.

[21]This assumption is not required for the arguments that follow.

[22]W. van Roosbroeck, Phys. Rev. 91, 282 (1953).

[23]Although the important quantities ρ_1^e and ρ_1^h are solved for inside the charge-neutral region using the Shockley technique, it should be noted that φ_1 cannot be found everywhere because no boundary conditions on φ_1 at $|x| = h - L$ are given.

[24]See A. Many, Y. Goldstein, and N. B. Grover, *Semiconductor Surfaces,* Ref. 7.

[25]A. S. Grove, *The Physics and Technology of Semiconductor Devices* (Wiley, New York, 1967).

[26]Interpretations of the surface-recombination velocity in terms of quasimicroscopic quantities such as capture cross sections, as, for example, in Ref. 25, clearly bear no relation to actual microscopic surface properties.

[27]Some attempts have been made, in the spirit of Refs. 7 and 26, to answer such questions; see, e.g., F. Berz, Proc. Phys. Soc. London 71, L275 (1958). As in Ref. 7, these are quasimicroscopic answers to macroscopic questions.

[28]In implementing (3.13) the assumption $d\rho_1^e/dx = -d\rho_1^h/dx$ is made. This, in effect, neglects a term $d^3\varphi_1/dx^3$, thereby lowering the order of the highest derivative of φ_1 from *three* to one.

[29]Mathematically, the situation here is akin to a singular perturbation problem (Ref. 4). The term "outer" is meant in that asymptotic sense.

[30]The validity of these assumptions can be checked *a posteriori.* (Quasimicroscopic arguments justifying these assumptions have been given in Ref. 25, p. 238. As usual, these arguments have no macroscopic significance.) Specific examples are given in Table I, where these assumptions have been checked and found well justified.

[31]See, for example, A. Many Y. Margoninski, E. Harnik, and E. Alexander, Ref. 8.

[32]There are two reasons why transient experiments do not permit outer-condition-type approaches. First, the (nonzero) charge-relaxation terms containing $E(t)$ and $H(t)$ produce additional contributions in (3.12) that prevent the reduction to (3.24), and second, J^e does not, in general, equal $-J^h$, as is necessary to reach (3.24). The former is dependent on the time rate of change of

carrier densities at the surface and, hence, will become negligible as the frequencies of the dominant Fourier components of the transient decrease (discussed further in Sec. IV). The latter is self-equilibrating in the sense that differences in currents build up surface charge, which tends to counteract and hence, equalize the contributing currents. Therefore, at some point after the initial rapid decay of the transient we can expect the two aforementioned effects to subside and that a quasi-dc outer condition analysis will become valid.

[33]A. Many and D. Gerlich, Phys. Rev. 107, 404 (1957).

[34]A. S. Grove, Ref. 25.

[35]Such effects have been discussed previously by A. S. Grove, B. E. Deal, E. H. Snow and C. T. Sah, Solid State Electron. 8, 145 (1965). Based on a specific quasimicroscopic interface model, they concluded that the effects of nonuniform dopant were insignificant. However, as we discuss later (see Fig. 8), redistribution effects are felt through the action of the surface electric field on the interface, an effect that was not included in their model. It is not clear whether their theoretical conclusion was ever tested experimentally.

[36]This is most easily seen if we neglect all logarithmic terms in (3.25) beyond the first. Then the fact that $(1+\rho_1^h/\rho_0^h)\ln(1+\rho_1^h/\rho_0^h)$ is always greater than ρ_1^h/ρ_0^h (except when $\rho_1^h \equiv 0$) implies our conclusion.

[37]To our knowledge, the non-small-signal regime has never been investigated systematically. The work of A. V. Rzhanov and I. A. Arkhipova, Fiz. Tverd. Tela (Leningrad) 3, 1954 (1961) [Sov. Phys.—Solid State, 3, 1424 (1961)] is of interest; however, the quasimicroscopic terminology of this work and the insufficient data published make any conclusions difficult.

[38]E. H. Nicollian and J. R. Brews, *MOS Physics and Technology* (Wiley, New York, 1982).

[39]No consideration of the lateral current flows often associated with inverted p-type MOS capacitors [see S. R. Hofstein and G. Warfield, Solid State Electron. 8, 321 (1965)] is given here. Also, *macroscopic* surface potential fluctuations (see Ref. 43), oxide-thickness variations, and other such effects, which would require a second dimension, are not considered.

[40]This simply requires that $\bar{\varphi}_1$ be sufficiently small. In Ref. 11 E. H. Nicollian and A. Goetzberger investigated the limits of small-signal behavior experimentally for particular samples (see their Fig. 11).

[41]Note that since the real and imaginary parts of $E(\omega)$ [or $H(\omega)$] are derived from the single real function $E(t)$ [or $H(t)$], they will be related by the Kronig-Kramers relations.

[42]We remark that the reduction to (4.29) and (4.30) is equivalent to simply ignoring the presence of holes in the problem from the start.

[43]It should be noted that if the fluctuations are on a macroscopic scale, then they may be incorporated in a macroscopic description. Their effects would be manifested as the result of spatial variations of surface coefficients whose surface averages would, in some sense, be the coefficients we discuss in a one-dimensional context. There remains some question of whether such spatial variations are macroscopically measurable and/or of any use for device-modeling purposes. If the fluctuations are on a microscopic scale, then, of course, they cannot be discussed within a continuum framework.

[44]A. C. Eringen, *Mechanics of Continua* (Wiley, New York, 1967).

[45]N. S. Saks, Solid State Electron 18, 737 (1975).

[46]This situation and the attendant difficulties often occur in the volumetric case, e.g., in treating general viscoelastic continua. For further information, see Ref. 48.

[47]H. G. deLorenzi and H. F. Tiersten, J. Math. Phys. 16, 938 (1975).

[48]B. D. Coleman, Arch. Rat. Mech. Anal. 17, 1 (1964).

[49]This procedure has been termed the principle of equipresence by Truesdell. See C. Truesdell and R. A. Toupin, in *Encyclopedia of Physics,* edited by S. Flügge (Springer, Berlin, 1960), Vol. III/1, Sec. 293.

[50]Since we wish to calculate only overall circuit parameters and not the detailed field dependence, fairly accurate results can be expected from this procedure.

[51]Obviously at lower frequencies the improved expression (B12) will be accurate. When $E(\omega)$ or $H(\omega)$ are important, we have no proof that this is the best choice for ρ_d^e. However, because it still is, at least, a reasonable choice, we are guaranteed that (B12) will be adequate at high frequencies.

[52]This is the usual depletion-layer approximation; e.g., see J. McKenna and N. L. Schryer, Bell Syst. Tech. J. 51, 1471 (1972).